Spring 2012

Finite element analysis of blade-formation interactions in excavation

Osei Brown

Department:

FINITE ELEMENT ANALYSIS OF BLADE-FORMATION INTERACTIONS IN EXCAVATION

by

OSEI FREMPONG BROWN

A THESIS

Presented to the Faculty of the Graduate School of the

MISSOURI UNIVERSITY OF SCIENCE AND TECHNOLOGY

In Partial Fulfillment of the Requirements for the Degree

MASTER OF SCIENCE IN MINING ENGINEERING

2012

Approved by

Samuel Frimpong, Advisor
Kwame Awuah-Offei
Grzegorz Galecki

ABSTRACT

The efficiency and costs of mining operations greatly depend on the efficient design and use of excavators. The performance of these capital-intensive excavators requires thorough understanding of the physical and design factors that affect the formation-cutting tool interaction process. The current body of knowledge, based on experimental and analytical methods, provides limited understanding of these factors, which limits the accurate design and performance of excavators. The soil constitutive equations used in most of the available finite element (FE) models also fail to adequately capture the elastic and plastic behaviors of soil formations. This research initiative uses FE techniques to model the soil-tool interaction phenomenon, with appropriate focus on the behavior of soils during excavation. This is a pioneering effort in developing FE model of the soil-dozer blade interaction using the modified Cam Clay elasto-plastic law. The model is validated with results from previous experimental and analytical methods.

The results provided soil forces, a progressive developed failure zone, displacement fields and stress distribution along the tool surface. The sensitivity analysis of changes in blade angle on cutting force showed that, the cutting force increases with increasing blade angle. The cutting depth of the blade had a similar effect on blade cutting force. Increasing the depth of cut increases the required cutting force. Increasing the coefficient of friction at the soil blade interface increases the blade cutting force. Reducing the coefficient of friction at the soil blade interface from 0.3 to 0.05 reduces the cutting force by 22.3%. The percentage represents the maximum potential savings in blade cutting force. This research initiative advances the frontiers of soil-tool interactions, during excavations, to expand the limited knowledge in this critical area.

ACKNOWLEDGMENTS

I want to thank my advisor, Dr. Samuel Frimpong, for all his guidance and encouragement throughout my program which has culminated into this thesis. All the financial support during the program is acknowledged and deeply appreciated.

I also want to acknowledge the enormous guidance and support received from my committee members – Dr. Kwame Awuah-Offei and Dr. Grzegorz Galecki. But for their keen interest and suggestions, this thesis report would not have reached its present state.

To the mother of the Mining Engineering Department at MS&T, Ms. Barbara Robertson, thank you very much for making my life as a student easier. Also, I am grateful for the insight, encouragement and friendship of my colleagues, James Otoo, Elijah Adadzi, Francis Arthur, Moagabo Mathiba, Muhammad Azeem Raza, Amirhossein Bagherieh, Siddhartha Agarwal and all the mining graduate students.

I am grateful to my cousin, Dr. Reynolds Frimpong, for his encouragement and advice throughout my education in the US. Finally, I want to thank my family for standing solidly behind me throughout the difficult times in my life. I say thank you very much and may God bless you.

TABLE OF CONTENTS

LIST OF ILLUSTRATIONS

Page

LIST OF TABLES

Page

NOMENCLATURE

Symbol	Description
τ	Soil shear strength
σ_n	Soil normal stress
c	Soil cohesion
Ø	Soil internal friction angle
γ	Soil unit weight
Q	Surcharge pressure acting vertically on soil surface
c_a	Coefficient of adhesion between soil and tool
d	Tool working depth
w	Cutting tool width
p’	Effective mean stress
q	Deviatoric (shear) stress
σ'_1	Major principal stress
σ'_2	Intermediate principal stress
σ'_3	Minor principal stress
v	Specific volume
e	Void ratio
λ	Slope of the normal compression line on $v - \ln p'$ plane
κ	Slope of swelling line on $v - \ln p'$ plane
N	Specific volume of normal compression line at unit pressure
M	Slope of the CSL in $p' - q$ space
$d\varepsilon$	Total incremental strain
$d\varepsilon_s$	Shear incremental strain
$d\varepsilon_v$	Volumetric incremental strain
$d\varepsilon_s^e$	Elastic shear strain
$d\varepsilon_s^p$	Plastic shear strain
$d\varepsilon_v^e$	Elastic volumetric strain
$d\varepsilon_v^p$	Plastic volumetric strain
f	Yield function of the MCC

p'_o	Pre-consolidation pressure (yield stress)
K	Bulk modulus
G	Shear modulus
μ	Poisson's ratio
Λ	Plastic consistency parameter
u	Element displacement vector
ε	Element strain vector
σ	Element stress vector
N_1	Linear interpolation function at node 1 of quadrilateral element
N_2	Linear interpolation function at node 2 of quadrilateral element
N_3	Linear interpolation function at node 2 of quadrilateral element
N_4	Linear interpolation function at node 2 of quadrilateral element
B	Dimension matrix of element
D^{ep}	Elastic and plastic constitutive matrix
F_e	External forces on element
V	Volume of element
K_e	Stiffness matrix of element
R	Internal element stresses
β	Coefficient of friction at soil-blade interface
a_o	Half of the preconsolidation pressure (yield stress)
α	Cutting angle (rake angle)
e_o	Initial void ratio

1. INTRODUCTION

1.1. BACKGROUND OF THE PROBLEM

The United States is a major mineral-producing country. US produces 78 major commodities and it is ranked among the top five countries in the global production of aluminum (10.5%), coal (20%), copper (8.4%), gold (11.7%), iron ore (4.8%), and silver (7.1%) (NMA, 2004; Tons et al., 2004). The US mining industry also produces significant aggregates and stones for construction and manufacturing. These minerals, aggregates, and stones form the foundation of the US economy in all major sectors and also provide a basis for technological advances. About 70% of all minerals and 90% of aggregates and stones in the US are extracted using surface mining technology. Excavation and loading are major primary operations in the surface mine production chain, constituting a significant component of the production cost (Tons et al., 2004). Thus, excavation and loading are important cost centers that need to be improved to lower production costs and improve overall energy efficiency.

Optimization of tool design will improve energy efficiency in earthmoving operations. Accurate modeling of soil-implement interaction is the basic key to this optimization. In most earth moving equipment, such as motor graders, scrappers and bulldozers, the working tool is a blade. Blade geometry and operating conditions, such as cutting speed, cutting angle, and cutting depth, have a great effect on machine productivity. The need for efficient and economic excavation requires thorough understanding of the mechanics of cutting tool-formation interactions.

Despite the relevance of understanding the mechanics of cutting tool-formation interactions, not much progress has been made in this frontier. This is because of the complicated nature of the process of interaction of a tool with a medium. The fact that the forces involved in excavating particulate material are functions of many parameters make the study of the subject quite complicated. The magnitude of this resistive force depends not only on the type of soil but on the size, shape and orientation of the cutting element. Moreover, part of this complexity is attributed to the fact that the behavior of the material during excavation is not yet well understood (Hemami et al., 1994).

During the last five decades, much research has been conducted on parametric studies for soil-tool interaction for modeling energy requirement of tillage and excavation operations using empirical methods (Payne, 1956; Aboelnor et al., 1998; Mouazen and Nemenyi, 1999, Rosa and Wulfsohn, 1999) and analytical (Osman, 1964; Reece, 1965, Mckyes and Ali, 1977; Perumpral et al., 1983; Swick and Perumpral, 1988). Empirical methods are very costly due to the instrumentation required to record data precisely. Also, these methods cannot be implemented at any desired time and place since providing required instrumentation may not be possible, and in most cases, empirical methods represent only regional conditions. Force models, developed from the passive pressure theory, have been successful to some extent. However, they can hardly be extended to a general case because of the underlying assumptions and simplification of tool shapes. With increasing computing power and development of more sophisticated material models, numerical simulation methods now show more promise in providing new and improved insights.

Constitutive stress-strain laws, or models of engineering materials, play a significant role in providing reliable results from any numerical solution procedure. Their importance has been enhanced significantly with the great increase in development and application of many modern computer-based techniques, such as the finite element, finite difference, and boundary integral equation methods. However, it has been realized that the advances and sophistication in computational solution techniques have far exceeded our knowledge of the behavior of materials defined by constitutive laws (Aboelnor, 2002). As a consequence, very often, results from a numerical procedure that may have used less appropriate constitutive laws can be of limited or doubtful validity. Hence selecting the correct or most appropriate available material model is of prime importance in achieving reasonable results from a numerical simulation.

1.2. STATEMENT OF THE PROBLEM

Excavators are widely used as primary production equipment in surface mining operations for removing overburden and ore materials. The efficiency and costs of mining operations greatly depend on the efficient design and use of these capital

intensive machines. Any naturally occurring formation is characterized by the defining properties of the constituent soils and rocks. These properties are shaped by the pre- and post-formation chemical and mechanical processes to yield the relative ease of digging or excavating the formation. Thus, an excavator's cutting force is a function of the formation properties, machine–formation interactions and the operating parameters of an excavator. The formation parameters include cohesion, internal friction angle, density, water saturation, formation hardness and compaction, abrasiveness, the angle of formation failure wedge, and shear plane angle. The machine–formation interaction parameters include adhesion and external friction angle. The operating parameters also include blade travel velocity, cutting angle, tool working depth beneath surface, and surcharge pressure acting vertically on formation surface. These defining characteristics must be controlled through optimization to yield efficient excavation (Frimpong and Hu, 2008). Accurate modeling of soil-implement interaction is the basic key to this optimization.

Modeling soil-tool interaction using finite element analysis produces some advantage over other modeling methods. In this case, any tool structure and the non-linear behavior of the cutting tool interaction can be modeled if a proper constitutive law is chosen (Kushwaha and Zhang, 1998). The finite element method (FEM) takes into account the effect of progressive and continuous cutting of the soil at the tip of the blade, with possible development of failure zones in the soil whenever the shear strength of the soil is exceeded. The solution provides detailed information on stress and deformation distribution fields in the soil, together with tangential and normal pressures developed at the blade soil interface. Also, the acting forces on the cutting tool are predicted (Yong and Hanna, 1977).

Soil mechanical behavior and soil-tool reactions are two aspects taken into consideration in finite element analysis of soil-tool interaction. Researchers have used different models to simulate soil mechanical behavior and the contact between soil and tool. Duncan and Chang's (1970) hyperbolic model has been used extensively for soil-tool interaction modeling (Chi and Kushwaha, 1989; Pollock et al., 1986; Bailey et al., 1984; Yong and Hanna, 1977). The advantage of hyperbolic elastic model is its simplicity. However, the major inconsistency of this type of model is that a purely

hypo-elastic model cannot distinguish between loading and unloading. In addition, the model is not suitable for collapse load computations (as in the case of excavation or cutting) in the fully plastic range. Potential numerical instability may occur when shear failure is approached (Schanz et al., 1999). The constitutive behavior of geomaterials can be effectively modeled in the framework of the elasto-plastic theory, as suggested by the main aspects of their mechanical response, such as strong non-linearity, irreversibility, pressure dependence, shear induced contractancy or dilatancy, volumetric hardening and softening. Asaf et al. (2007) during their research for defining required parameters for soil simulation found that it is required to use elastoplastic relationships to increase accuracy and to minimize error to less than 15%. In analysis with elastoplastic models, Drucker-Prager's elastic-perfectly plastic model (Drucker and Prager, 1952) is used (Araya and Gao, 1995; Davoudi et al., 2008). The Drucker-Prager (1952) model is mathematically simple and easy to implement in a computer code. However, the model is not accurate for general stress paths, especially for highly frictional soil (Brinkgreve, 1994). Also, it cannot predict plastic volumetric strain or compaction of soil; an important property of soils. There is therefore the need to use an elastoplastic model that can deal with the various issues associated with modeling soil mechanical behavior in soil-cutting tool interaction.

The effective handling of the challenges in formation-machine interaction modeling is the key factor that will ensure machine operating efficiency. Thoroughly understanding the factors that affect the soil-cutting tool interaction will result in efficient and effective use of excavating machines for increased productivity and reduced maintenance and operating costs.

1.3. OBJECTIVES AND SCOPE OF THE RESEARCH

It is clear from the above discussions that for earth moving equipment, soil-machine interaction is an important phenomenon. Achieving higher performance of these machines can be done through an investigation of the physical and design factors that affect the soil-tool interaction process. This work seeks to advance existing knowledge

and frontiers in machine-formation interaction by using an elasto-plastic soil constitutive model in the finite element formulation. The primary objectives of this study are to:

- Develop a finite element model of the soil-cutting blade interaction using the MCC elasto-plastic law, and;
- Study different factors affecting the soil-cutting tool interaction process.

The study is limited to a wide cutting blade, such as that of a bulldozer, which has a width to depth of operation ratio greater than two (2). In such cases, the strains in the third dimension can be assumed to be negligible and hence can be ignored. A plain strain condition for 2-D models is thus used in this approach.

1.4. RESEARCH METHODOLOGY

The study combines the use of analytical literature review, numerical modeling and detailed analysis of simulation results to achieve the research objectives. The detailed literature survey is used to establish the body of knowledge in the field. The survey is also used to assess the suitability of existing modeling techniques and soil constitutive stress strain laws.

Finite element (FE) modeling techniques are used to study the behavior of formation-blade interactions in excavation. The mechanical behavior of the soil is modeled as a non-linear elasto-plastic material using the Modified Cam Clay. Coulomb friction model is used to describe friction at the soil-blade interface. The geometry and meshing of the finite element model is generated using HyperMesh (Altair HyperWorks, 2009). Simulation and post-processing of the model is performed with the finite element commercial package ABAQUS (2010). An incremental method based on the single-step Newton iteration algorithm is used to solve the finite element equilibrium equations. The developed FE model is validated by qualitatively comparing the results from the analysis and to previous experimental, as well as numerical methods.

Detailed analysis of the simulation results is carried out to investigate the interaction between the cutting blade and soil. Also studied, are the effects of the cutting blade operating conditions and soil-blade interface property on machine performance.

1.5. RESEARCH CONTRIBUTIONS

This research study contributes to the existing body of knowledge and advances the frontiers in formation failure mechanics and machine-formation interaction using numerical modeling techniques. The research is a pioneering effort in developing a finite element model of a soil-cutting blade using the Modified Cam Clay (MCC) law (Roscoe and Burland, 1968). The MCC is a non-linear strain hardening model, which models the elastic and plastic behavior of the soil by means of hardening plasticity. The model is based on critical state soil mechanics.

The study provides information on the effects of cutting blade operating conditions and soil blade interface property on machine performance. This information will aid industry in the efficient and effective use of excavating machines (bulldozer) for increased productivity and reduced maintenance and total operating costs. The results of the research will also be useful to the equipment manufacturing industry for appropriate design modification. This research effort has resulted in one refereed journal and two conference publications with a potential for additional publications, which forms a basis for expanded research in this area.

Another very important application of this research is in excavating machine simulators that are employed for training equipment operators. It is cost effective to train an operator on a simulator before he gets on to the real machine. The finite element model can be integrated with such software. In this way, when the operator trainee runs the cutting tool (blade, bucket, etc.) through the soil or fragmented rock, the software recognizes a resistance from the formation.

1.6. STRUCTURE OF THESIS

Following the introduction section in Chapter 1, a comprehensive review of all relevant literature is presented in Chapter 2. Different methods used in studying soil-tool interaction are presented with their merits and limitations. The Chapter also contains a description of soil properties, critical state soil mechanics and the Modified Cam-Clay (MCC) soil constitutive model. Chapter 3 presents the numerical modeling of the soil-

blade interaction. It contains the mathematical framework of the MCC and the FE formulation of the soil blade interface problem. The model validation and experimentation program adopted in this research are also presented in Chapter 3. Chapter 4 contains the results of an extensive study of the soil-tool interaction process. Major conclusions of the study and relevant recommendations for future work in this research paradigm are covered in Chapter 5. The bibliographic list obtained from an extensive literature review is given in the references section.

2. LITERATURE SURVEY

An extensive literature survey of soil mechanics and different approaches for soil-tool modeling is the focus of this chapter. This is necessary to investigate the dynamics of soil-tool interaction. The Chapter will focus on three main areas including: (i) Present brief description of soil properties and behavior relevant to the study; (ii) Review the available models of studying soil-tool interaction; (iii) Present the background theory of the critical state soil mechanics and the overall overview of the Modified Cam-Clay model.

2.1. SOIL PROPERTIES AND BEHAVIOR

A good understanding of soils and their properties and behavior based on experimental observation is important for reasonable simulation of the soil behavior and hence for the overall soil-tool interface process.

2.1.1. Nature of Soils. Soils are the product of physical and chemical weathering of rocks. Physical weathering includes climatic effects such as freeze-thaw cycles and erosion by wind, water, and ice. Chemical weathering includes chemical reaction with rainwater. The particle size and distribution of various particle sizes of soil depend on the weathering agent and the transportation agent. Soils are categorized as gravel, sand, silt, or clay, depending on the predominant particle size. Gravels are small pieces of rocks. Sands are small particles of quartz and feldspar. Silts are microscopic soil fractions consisting of very fine quartz and other minerals. The average size of solid particles ranges from 4.75 to 76.2 mm for gravels and from 0.075 to 4.75 mm for sands. Soils with an average particle size of less than 0.075 mm are either silt or clay or a combination of the two (Terzaghi et al., 1996).

Soils can be divided into two major categories: cohesionless and cohesive soils. Cohesionless soils, such as gravel, sand, and silt, have particles that do not adhere (stick) together even with the presence of water. On the other hand, cohesive soils (e.g. clays)

are characterized by their very small flakelike particles, which can attract water and form plastic matter by adhering (sticking) to each other.

2.1.2. Soil Parameters. The behavior of a soil in the field depends not only on the significant properties of the individual constituents of the soil mass, but also on those properties that are due to the arrangement of the particles within the mass. Accordingly, it is convenient to divide index properties into two classes: soil grain properties and soil aggregate properties. The principal soil grain properties are the size and shape of the grains and, in clay soils, the mineralogical character of the smallest grains. The most significant aggregate property of cohensionless soils is the relative density, whereas that of cohesive soils is the consistency (Terzaghi et al., 1996). Soil behavior is significantly controlled by its micro-scale properties. However, the overall response of the soil aggregate to induced load is of greater interest.

2.1.2.1 Porosity, void ratio and relative density. Porosity is the ratio of the volume of voids to the total volume of the soil aggregate. Void ratio is the ratio of the volume of voids to the volume of the solid substance. The porosity of a natural sand deposit depends on the shape of the grains, the uniformity of grain size, and the conditions of sedimentation. Although porosity is greatly influenced by the shape of grains and the degree of uniformity, porosity itself does not indicate whether a soil is loose or dense. This information can be obtained only by comparing the porosity of a given soil with that of the same soil in its loosest and densest possible states. The looseness or denseness of soil can be expressed numerically by the relative density (Tarzaghi et al., 1996). The compressibility and strength of a granular soil are related to its relative density, which is a measure of the compactness of the soil grains.

2.1.2.2 Moisture content. Moisture content is one of the main factors affecting the resistance of soils to deformation. The moisture content is determined by the quantity of water contained in the pores. Depending on the quantity of water, the properties of the same soil change significantly. With increase in the moisture content of cohesive soils,

the coefficients of friction and adhesion decrease and the soil shows lower resistance to external loads (excavator bucket or blade force) (Zelenin et al., 1985).

2.1.2.3 Plasticity and consistency. This is the capacity of a material to change its form without a change of volume. In a certain range of moisture content, all cohesive soils exhibit plasticity. The more the finely dispersed clay particles in the soil, the higher its plasticity. Cohesive soils are found in the plastic state when the limits of their moisture content correspond to the plastic and liquid limits.

The concept that the moisture content of a fine-grained soil profoundly influences the state in which that soil exists is expressed through the consistency limits and related indices (Karafiath and Nowatzki, 1978). It is the degree of mobility of soil particles at different moisture contents due to mechanical action on the soil. The compact state of cohesive soils depends upon consistency, that is, their compactness. By comparing the natural moisture content of soil at the liquid and plastic limits, the following states of soils can be distinguished:

1. When the actual moisture content is more than the liquid limit, the soil has a liquid consistency and has the properties of a viscous fluid;
2. When the actual moisture content is within the plastic and liquid limits, the soil is in a plastic state and deforms plastically without breaking;
3. When the natural moisture content is less than the plastic limit, the soil is in a solid state (Zelenin et al., 1985).

The behavior of soils under load has been studied in detail in relation to some engineering problems: soil under foundations or in construction of supporting walls or embankments. In all these forms of construction, the stresses developed in the soils should not exceed the elastic limit. With the appearance of plastic (irreversible) deformations, emergency situations, such as sagging of erected constructions arise. Soil mechanics is mainly based on the theory of elasticity. As a result, it can be successfully applied to many engineering problems.

During the interaction of working tools of machines with soil, stresses exceeding the elastic limit develop in the soil. The stresses reach a maximum (limiting) value in the

region of plastic deformation of the soil. In the process, the soil is loosened with a total loss of structural strength and some volume is separated from the massif.

Thus, the assessment of the loosening capacity of the soil by using the theory of elasticity from soil mechanics is not applicable in describing the process of loosening of soils during excavation by machines. Irrespective of the degree of deformation of the medium and in any complex stress condition, fracture in a brittle material can occur only due to tension and that in plastic materials due to shear. All cohesive soils (and such soils are predominant) constitute a plastic medium, the fracture of which occurs due to shear stress.

Knowledge of the resistance of a soil to failure in shear is required for analyzing of the stability of soil masses. If at a point on any plane within a soil mass the shear stress becomes equal to the shear strength of the soil then failure will occur at that point (Zelenin et al., 1985).

2.1.2.4 Shear strength of soil. The shear strength of a soil is its resistance to deformation by continuous shear displacement of the soil particles upon the action of shear stress. When the maximum shear stress is reached, the soil is regarded to have failed. The failure conditions of a soil may be expressed in terms of limiting shear stress, called shear strength, or as a function of principal stresses. The shearing resistance of soil is constituted of the following main components (Kumari, 2009): (i) the structural resistance to displacement of the soil due to the interlocking of the particles; (ii) the frictional resistance to translocation between the individual soil particles at their contact points; and (iii) cohesion or adhesion between the surfaces of the soil particles.

The shear strength in cohesionless soil results from inter-granular friction alone, while in cohesive soils it results both from internal friction as well as cohesion. Figure 2.2 shows the strength characteristics of soil with different compaction densities.

Strength is the measure of the maximum stress state that can be induced in a material without it failing. The shear strength of a soil is indicative of the stability and strength of the soil under various conditions of loading, compaction, and moisture content. However, the shear strength of a soil, determined experimentally is not unique. It can vary depending on the method of testing. Shear strength parameters are very

important for stability analyses. Soils with high shear strength will be able to support structures without failing. Otherwise, the structure will not be stable and premature failure will occur, either, in the short term or long term depending on the shear strength (Anim, 2010).

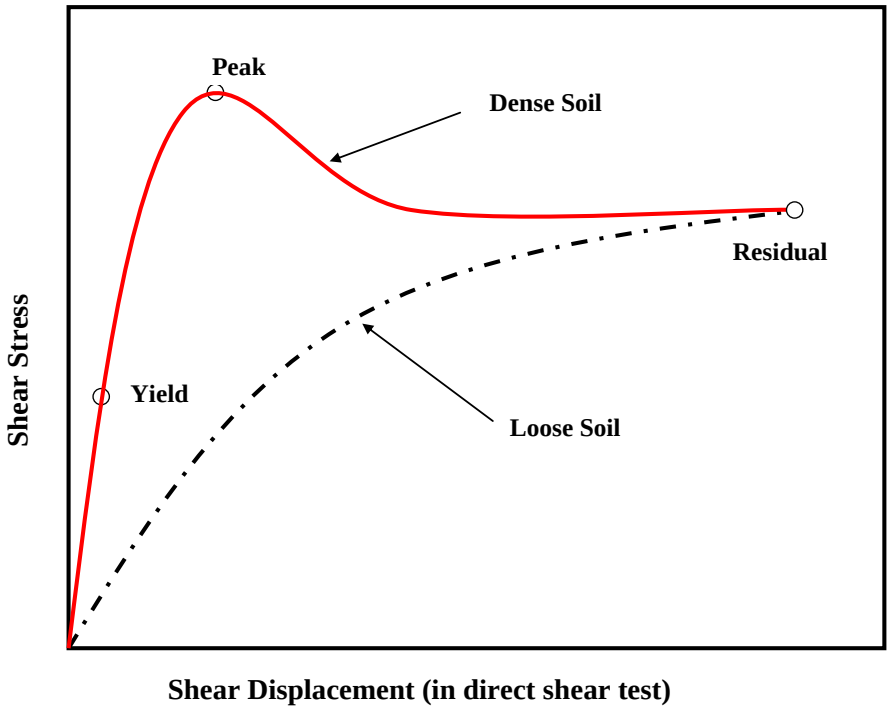

Figure 2.1 The strength characteristics of soils with different compaction densities

When shear stress is applied, the resulting deformation is always accompanied by a volume change, which is known as dilatancy. This shear-induced volume change accrues as a result of two competing modes of particle movement, namely, slip-down and roll-over (Dafalias, 1993). Figure 2.3 illustrates vertical displacement of soil measured during direct shear test. The slip-down movement of grains tends to reduce the volume by repacking the soil into a denser state. This mechanism is activated largely in loose deposits of soil. The roll-over mechanism tends to increase the volume which is characteristic in the behavior of dense soil.

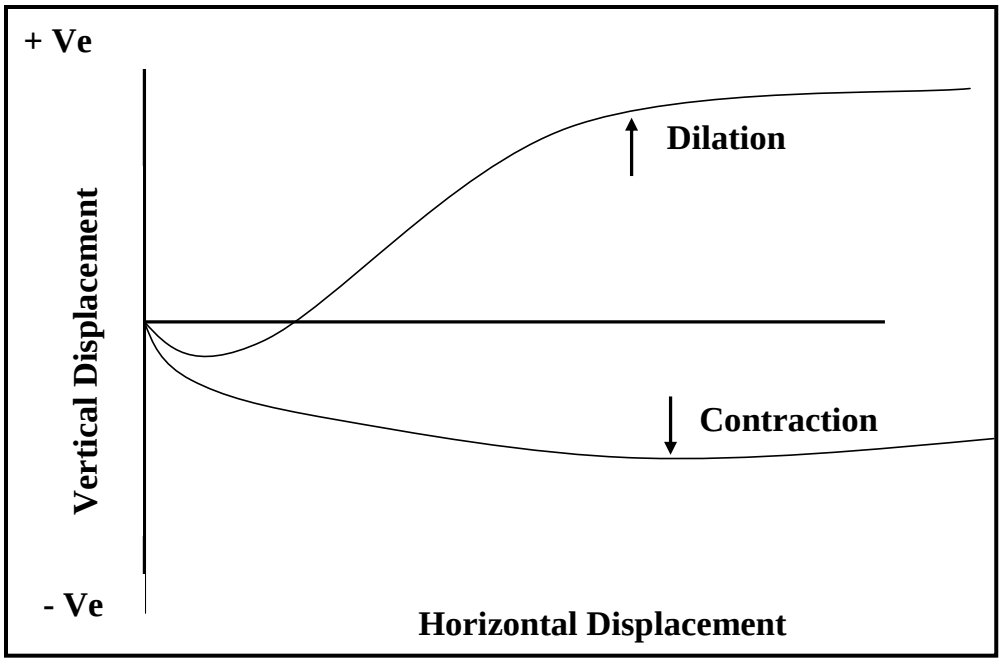

Figure 2.2 Vertical displacement of soil measured during shearing

When slip-down takes place, particles are filling gaps in the void and not moving largely in the direction of shearing. Therefore, the slip-down movement can occur rather easily without mobilizing a large amount of shear strain and the volume reduction is generally observed at an early stage of loading in the tests on sands with a wide range of density. A larger movement is always required for particles to roll over neighboring ones and hence the volume increase or dilation is generally induced at a later stage of shear stress application where the soil is largely deformed.

For soil with high density, the soil tends to exhibit strain hardening accompanied with dilatational behavior. The shear stress goes up initially, passes a peak stress and then softening behavior starts, leading to a residual strength. However, for soil with low density, the strain-hardening behavior is exhibited with no post-peak softening.

Shearing resistance in soils is the result of resistance to movement at interparticle contacts. Each contact can transmit normal force from one particle to another across an area that increases or decreases as the normal force increases or decreases. Shearing resistance of soils is created when bonds are formed across the contact areas of particles and the particles interlock each other. Tangential or sliding movements of the soil

particles are as a result resisted. All these bonds increase with increasing interparticle contact area. Therefore, any mechanism that increases interparticle area contributes to shearing resistance.

2.1.2.5 Volumetric response of soils during shear. Density, effective stress, and soil structure are the three important variables that determine the shearing resistance of soils. It is a distinctive characteristic of soils that, during the mobilization of shearing resistance, shear deformation is accompanied by a change in either density or effective stress. Furthermore, the nature and magnitude of this change depend on the pre-shear density and effective-stress condition, as well as the soil structure. The mechanism responsible for a volume or porewater pressure change is the tendency of soil particles to rearrange themselves during shear. If water can leave or enter the soil, the tendency for particle rearrangement manifests itself as a change in volume and, consequently, in density. If volume change is not possible, the porewater pressure change produces a change in effective stress. Soils of low pre-shear density, such as loose sands and silts and soft clays, tend to compress during shear. On the other hand, soils of high densities (dense sands, gravels, stiff clays and shales) tend to expand. However, as the pre-shear effective confining pressure increases, the tendency for volume increase is suppressed (Terzaghi et al., 1996).

2.2. METHODS OF SOIL – TOOL INTERACTION MODELING

In excavation, the cutting tool (blade in a case of a bulldozer) encounters a resistance force from the formation that must be overcome in order for the tool to penetrate into or cut through the medium. This force must be provided by the driving elements/actuators on the excavating machine (Hemami and Hassani, 2007). The resistance from soil on a cutting tool forms the basis of the theory of cutting resistance on excavation machines (Awuah-Offei, 2005). It is key to modeling the total force on the cutting tool (blade, bucket or dipper) during excavation.

Studies of soil-tool interaction have been carried out mostly for the development of force prediction models using different soils, tools, and operating conditions (speed

and depth of operation, and tool orientation). The formation of 2D and 3D soil failure patterns have been taken into account. So far, three (3) major methods, namely experimental, analytical and numerical methods, have been used to solve problems in the area of soil-tool interaction and failure mechanism (Shen and Kushwaha, 1998).

Most of the experimental studies previously done were mainly carried out for the verification of either mathematical (Reece, 1965, Mckyes and Ali, 1977; Perumpral et al., 1983; Swick and Perumpral, 1988) or finite element (Yong and Hanna, 1977; Mouazen and Nemenyi, 1999; Abo-Elnor, 2003) models. The advantage of the experimental method is that researchers can obtain first-hand experience on performance evaluation of different tools. Since the physical conditions in fields are continuously changing, it is difficult to determine the basic rules governing soil-tool interaction from such experiments conducted during a specific period of time and at a single location. Moreover, experimental study of soil–blade interaction is expensive and may be limited to certain cutting speeds and depths. Results are also highly dependent on the accuracy of the measuring devices (Abo-Elnor, 2003).

2.2.1. Analytical Methods. Analytical approach is one of the first methods for predicting the interaction between soil and a cutting tool. This approach has been used by many researchers, especially in the field of soil tillage for about five (5) decades. The results of this approach are still valid to some extent and its governing rules are sometimes used in different approaches, such as experimental and numerical approaches.

The limit equilibrium[1] is one of the most important analytical approaches used in soil tool interaction. The basic idea behind it is that soil and tool (or machine) are considered as a whole. The force equilibrium equations over the entire system are established with soil being in its limit state where its resistance becomes largest. From the equilibrium equations, forces acting on a tool or machine can be solved. In general, the basic assumptions for a limit equilibrium method include (Shen and Kushwaha, 1998):

1. The soil is considered as a rigid material, that is, it is not deformable.

[1] The limit equilibrium as discussed in this work is for soil-tool interaction problems that are solved analytically, and that the method can also be applied to complex problems which require numerical solution.

2. The soil might fail inside the soil body and/or at a soil - metal interface. For the failure inside the soil body, one or several parts of soil may slide over a potential failure surface while with the failure at the interface, soil may slide over a metal-soil interface.
3. The pattern of one or more failure surfaces inside the soil body is assumed or predetermined on an application-dependent basis. Many patterns have been proposed by different investigators in the past. Each pattern may involve one or more unknown parameters leading to a series of potential failure surfaces. The unknown parameters are determined by performing an optimization to find the most critical failure surface which generates a minimum reaction force to a tool or machine.
4. The forces interacting on a failure surface in the soil body are determined by the Mohr-Coulomb criterion.

Two most important factors in this approach are:

1. Shape of soil failure surfaces: The shape is normally proposed on the basis of empirical observation or data, and is very crucial to the success in applying the limit equilibrium to an analysis of soil-machine systems.
2. Equilibrium equations: For two dimensional cases, the equilibrium equations in horizontal and vertical directions can be established by considering each individual soil block separated by failure surfaces in the soil body or soil-metal interfaces. For 3D cases, the equilibrium equations are set up in lateral, longitudinal and vertical directions. Solving these equations provides useful force information in a soil-machine system such as the cutting or penetration force of a work tool.

The differences in the shape of the failure surfaces assumed or predetermined is the basis for the numerous cutting force models available. The limit equilibrium method provides only the information about the maximum forces generated within the soil. However, the method does not provide any information on the deformation of the soil. This is due to the fundamental assumptions embedded in the limit equilibrium. These

assumptions make the method of a very simple form but quite limited in the power of analyzing the deformation in the system (Shen and Kushwaha, 1998).

The first significant theoretical model to predict the resistance of a soil media to shearing stresses was proposed by Coulomb. The Coulomb failure theory defines failure in terms of stress conditions contrary to those based on strain. The Coulomb yield criterion defines failure to occur in a material when the shear stress on any plane equals or exceeds the shear strength of the material on that plane. Shear strength is itself a function of the normal stress on that plane as illustrated in Equation (2.1) (Terzaghi et al., 1996).

$$\tau = f(\sigma_n) \tag{2.1}$$

Coulomb (1776) defined $f(\sigma_n)$ as a linear function of the normal stress. The linear function has the advantage that computations of shear strength can be made readily and for most soils it describes the relationship between strength and normal stress adequately. The linear form of the Coulomb expression is given in Equation (2.2).

$$\tau = c + \sigma_n \tan\emptyset \tag{2.2}$$

Osman (1964) first used the passive pressure theory on large retaining walls to study the mechanics of 2D soil cutting blades. Osman considered the case of a wide cutting blade taking into account rake angle, soil properties, surface roughness of the cutting blade, and also the effect of curvature. A curved failure surface is more realistic in excavating than the flat surface assumed by other models. However, improvement in the models when the curved failure assumption is used is not significant enough to justify the mathematical difficulty (Wilkinson and DeGennaro, 2007). The total force on the blade was divided into two parts by: (1) Treating the soil as frictional and heavy, but with no cohesion nor surcharge, and (2) Treating the soil as weightless but frictional, with cohesion and surcharge.

Reece (1965), proposed Equation (2.3) as the universal earthmoving equation (UEE) for describing the force necessary to cut soil with a tool using the grouping of Osman (1964).

$$F = \left(cdN_c + \gamma d^2 N_\gamma + QdN_Q + c_a dN_a\right)w \qquad (2.3)$$

The four (4) terms of Equation (2.3) in brackets represent the effects of soil's cohesion, its weight, any surcharging load that is present, and the adhesion that develops between the soil and the metal parts of the machine. The N factors are dimensionless numbers describing the shape of the soil failure surface. They, therefore, depend on the friction angle, angle of soil-to-metal friction and the shape of the structure and soil mass involved in the system. The N factors can be determined analytically for simple cases of tool and soil combinations. However, it is not yet completely known for what complexity of tool shapes the N-factors can be determined, analytically.

Payne (1956) conducted a series of qualitative experiments to observe the behavior of soil under the influence of vertical narrow tines. A failure zone which includes a triangular center wedge, a center crescent and two side blocks (Figure 1) was proposed based on the observed pattern of cleavage in front of the tillage tool. Based on the forces acting on the failure zone in front of the cutting tool, a force model was proposed by assuming that soil failure along soil-soil planes are governed by Coulomb failure criterion (Equation 2.2). One limitation of this model is that the procedure for calculating the forces on a tool is complicated and time consuming. Changes in the geometry of the tool such as rake angle, depth and width were observed to cause a change in the shape of the wedge ahead of the cutting tool (Payne and Tanner, 1959).

McKyes and Ali (1977) realized that the available models for predicting the forces acting on a narrow soil cutting blade have required separate measurements of the shape of the three-dimensional soil failure pattern ahead of the blade. They proposed a 3D failure profile consisting of straight line failure patterns in the soil. The failure profile was used to predict both the draft forces and the volume of soil disturbed in front of a narrow blade. Limit equilibrium mechanics equations were written for the soil wedges in terms of an unknown angle of the failure zone and the theoretical draft force was

minimized with respect to this angle. The proposed draft equation is similar to the universal earth equation proposed by Reece (Equation 2.3). The N factors were however, computed for a 3D soil failure.

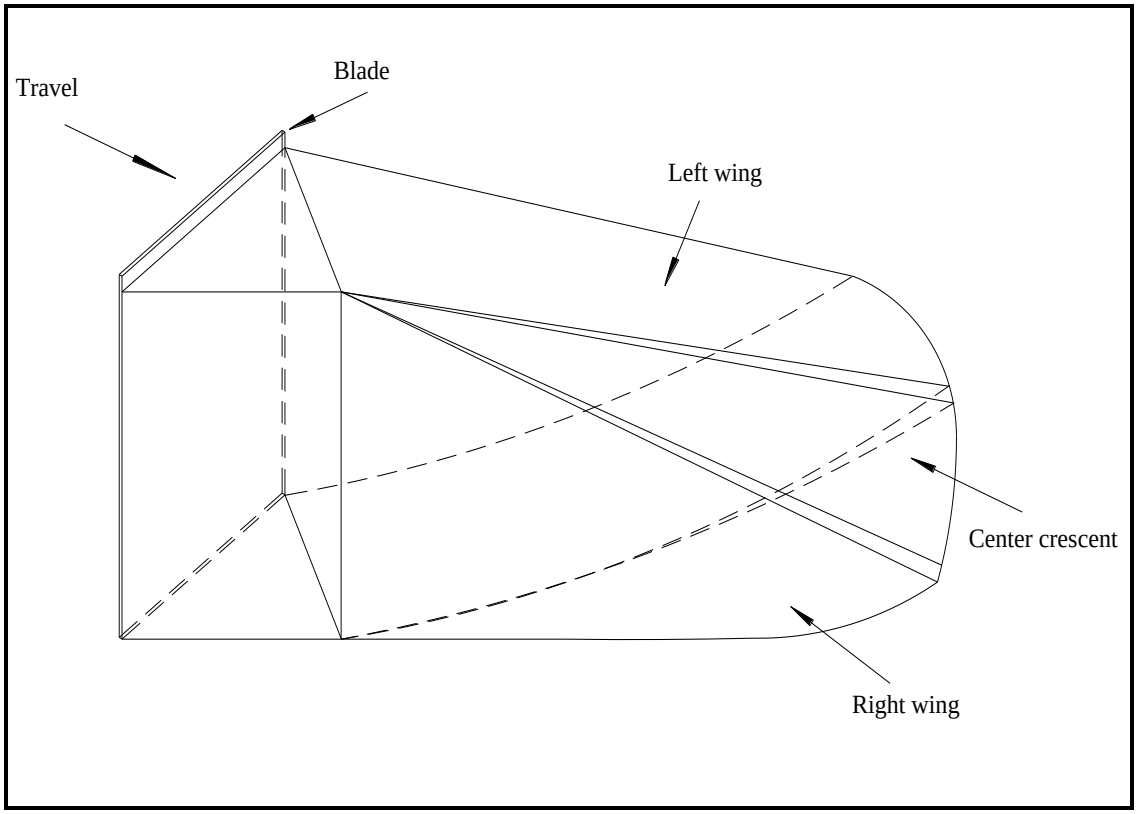

Figure 2.3 Failure zone of Payne model (Payne, 1956)

Perumpral et al. (1983) replaced the side cresents of the failure pattern ahead of the blade with a set of forces on either side of the center wedge for simplicity. Also, a plane surface was assumed for the curved sliding surface. The model developed was similar to that developed by Ura and Yamamoto (1978) for predicting the behavior of anchors in sand. One major difference was that, the effect of cohesional and adhesional characteristics of the soil were included in the tool model.

The models discussed above were developed under quasi-static conditions without taking the dynamic effect into consideration. To account for the dynamic effect,

Swick and Perumpral (1988) modified the model developed by Perumpral et al. (1983). A major step in modifying the static model to a dynamic model included incorporation of terms that accounted for the acceleration force. A modification of the acceleration force equation developed by Soehne (1956) was used for this purpose. The acceleration force, acting parallel to the rupture surface, was represented as a body force resisting acceleration of the wedge. Swick and Perumpral (1988) evaluated their model against indoor soil bin test results. The tests were conducted in an artificial soil using four tine widths, three operating depths, three rake angles, and four forward speeds. The model predictions were in reasonably good agreement with laboratory test results. Although the model allowed for strain rate effects on shear stress, shear rate did not influence either soil shear strength parameters or soil-metal friction significantly. Inertial forces accounted for most of the increases in tool forces observed under dynamic conditions.

The models discussed above serve their purposes to a certain extent. However, the methodology for developing these models has the following intrinsic weaknesses (Shen and Kushwaha, 1998):

1. A failure profile is a prerequisite for the limit equilibrium analysis. However, the choice of the assumed profiles is arbitrary and depends on each particular investigator.
2. Soil mechanical properties are assumed to be uniform without considering layered characteristic of some formations.
3. The mode of soil failure is affected by the tool speed. It is difficult to define such influence by tracing or describing the failure profile, a variant with the speed.
4. Soil velocity and acceleration profiles in front of a tillage tool have to be simplified and assumed to follow a simple pattern without justification.

Evidently, the above weaknesses may introduce errors in calculating forces in soil-tool interaction, especially in the cases different from the soil and tool conditions under which the model was developed. Therefore, the use of the analytical models, based on passive earth pressure theory and assumptions of a preliminary soil failure pattern, is limited for optimum machine design. Hence, it is important to have a method that can alleviate these weaknesses to a certain extent.

2.2.2. Numerical Simulation of Soil-Machine Interaction. Zeng and Yao (1992) questioned the neglect of the dynamic effects by classical passive earth theory models and the use of the limiting stress condition of Coulomb materials. These assumptions, they contend, applies only to those soils that provide definite failure profiles and not flow failure soils. The passive earth theory and similar models were built on the assumption that soil failure is instantaneous along the entire failure plane. Although this may be true for plastic soils, not all soils fail in this mode.

The need for soil cutting models that allow for progressive soil failure led to the use of numerical methods in soil-tool interaction modeling. Until the advent of electronic computation, engineering processes studied were drastically simplified so that the governing equations could be solved analytically. Over the last three decades, however, computers have made it possible, with the help of suitable mathematical models and numerical methods, to solve many practical problems of engineering. There are several reasons why the use of numerical methods has gained growing popularity:

1. Most practical problems involve complicated domains (both geometry and material constitution), loads, and nonlinearities. These problems require rigorous theoretical and numerical solutions, which are not tractable using analytical solutions.
2. Numerical modeling can be used to investigate the effects of parameters, such as geometry, material parameters, or loads, on a system on its response to gain a better understanding of a process / system. It is cost effective and saves time and material resources compared to the amount of physical experiments required to gain the same level of understanding.
3. It is possible to include all relevant features in a mathematical model of a physical process without solving the model by exact means.

So far, about two major numerical methods, namely finite element method (FEM) and discrete or distinct element method (DEM) have been used to solve problems in the areas of soil-tool interaction and failure mechanism.

2.2.2.1 Discrete element method. Cundall and Strack (1979) introduced the concept of DEM in the analysis of discrete assemblies. The method was applied to analyze the motion and forces of an assembly of discs. In this method, the interaction of the particles is viewed as a transient problem with states of equilibrium developing whenever the internal forces balance (Cundall and Strack, 1979). The equilibrium contact forces and displacements of a stressed assembly of particles are found through a series of computations tracking the movements of the individual particles within each time step. Within each time step, the velocities and acceleration are assumed to be constant. The computations are made fairly easy because it is assumed that the time step is small enough so that a disturbance cannot be propagated beyond the immediate neighbors.

Tanaka et al. (2000) applied this numerical method to model the deformation and resistance forces of soil as a tool moves through it. The initial predictions were flawed necessitating changes in the original model. Tanaka et al. (2000) attributed the flaws to the rigidity of the model particles and the mechanical parameters (including spring and damping constants) used in the model. To verify this, they used rigid balls of alumina instead of soil in the tests. The deformation predictions improved when compared to the assembly of alumina balls instead of soil but the resistance force predictions did not.

Momozu et al. (2003) introduced a modified version of the DEM to model a soil loosening process using a pendulum-like cutting tool. They introduced a tensile force between the elements. This tensile force accounted for the attraction between soil particles which prevents them from behaving like rigid balls (like the alumina balls of Tanaka et al., 2000). Even though the resistance forces were not computed, the modified DEM had better predictions of the deformation pattern.

The existing applications of the DEM have concentrated on attempts to model soil samples in a container (Tanaka et al., 2000) and as a block of soil (Momozu et al., 2003). Given the large numbers of particles during excavation, the current state of the DEM techniques seems incapable of solving these problems even with the resolution of the force predictions (Awuah-Offei, 2005).

2.2.2.2 Finite element method (FEM). The finite element method originated from the need for solving complex elasticity and structural analysis problems. Any numerical method of soil failure modeling including FEM has to use a constitutive model to describe the relationship between applied stresses and resultant strains within the soil. Linear and nonlinear models have been categorized based on using a linear or nonlinear equation to relate stress and strain within the soil. Based on the theory of plasticity, soils can also be viewed as only elastic, or purely plastic, or both elastic and plastic materials during the loading process. And finally, soil is viewed statically or dynamically depending on the influence of time on its behavior. Much work has been reported on the static or dynamic analysis of soil-tool interaction in tillage/earthmoving operations using the FEM.

Yong and Hanna (1977) opened a new era in the analysis and design of the tool or machine in a soil-machine system, by applying the FEM in analyzing the soil-cutting process. They modeled the interaction between a wide blade and soil. A plane strain condition (i.e., no strain in the direction of blade width) was assumed, which is reasonable for wide blades except at the edge of the blade. The developed FEM takes into account the effect of progressive and continuous cutting of the clay soil at the tip of the blade, with possible development of failure zones in the soil whenever the shear stress exceeds the shear strength of the soil. The solution provides detailed information on stress and deformation fields in the soil, together with tangential and normal pressures developed at the blade soil interface.

Kushwaha and Shen (1995) used FEM to solve the dynamic equation of interaction between the soil and a tool, which was previously used for the similar cases. By using a 2D FEM, it became possible to predict the draft requirement of a vertical blade on soil. Comparison between the results of soil bin tests and the modeling showed that the predicted draft was very close to the experimental data. It was indicated that the method could work for predicting the forces acting between the soil and any other kinds of tillage tools by some modifications.

Finite element method was implemented by Rosa and Wulfsohn (1999) to study a constitutive model for high speed tillage by using narrow tillage tools. Two different tools, including a flat and a triangular edged narrow tool, were used for soil bin

experiments to test the effect of forward speeds between 0.5 to 10.0 m/s over a distance of 1 to 3 m. The model's assumptions included: (1) Narrow and rigid tool working in constant depth and velocity; (2) Failure is a 3-D case; (3) Negligible tool deflection compared to the soil deflection; (4) Totally smooth or totally rough soil-tool interface for simulating extreme cases; (5) Isotropic and homogeneous soil medium; and (6) Soil particles are lumped masses and gravity effects are negligible compared to the inertial and strain rate effects or the contributed soil stiffness to draft. The predicted draft was less than 1% over the measured value at a tool speed of 2.8 m/s but was 25% more at a speed of 8.4 m/s. Simulation results indicated that draft of the triangular tool was less than that of the flat tool, and that the draft of the elliptic tool was less than that of the triangular tool at higher speeds. Since the elliptic tool required less draft than the triangular tool, the authors felt that remolded soil behaved like a viscous fluid and the drag effect dominated the draft response compared to the effect of soil strength or soil stiffness.

Chi and Kushwaha (1991) used a non-linear 3-D FEM to investigate soil-tool interaction. One of the main goals of this research was the evaluation of the effect of draft requirements of tillage tools on wear and friction losses. Actual tests in the soil bin were conducted to compare with the results of the model. Draft was measured for different rake angles of the tool. Results of both theoretical and experimental methods obviously showed that the draft requirement decreased as the rake angle decreased, but stayed constant for the rake angles less than 45°. Results were very close, showing only about 0.8% error for a rake angle of 45° and 10.5% error for a rake angle of 90° when compared with actual test results of the soil bin. The tool edge stress was very large, and the maximum stress increased with increasing depth. Thus, the outer edges of the tool at the bottom suffered the greatest stress and wear. As well, this stress increased with increasing rake angle. Since the vertical position of the tool required the highest draft, it showed the highest level of the stress.

To date, only few studies have focused on real tillage implements using FEM to investigate the forces interacting between soil and tillage tools. Mouazen and Nemenyi (1999) developed a 3-D finite element model for the interaction of a subsoiler with a chisel point operating in a non-homogenous sandy loam soil. The soil was modeled using

8-node brick elements and was assumed to behave like an elastic-perfectly plastic material. The Drucker-Prager yield criterion with the associated flow rule was assumed. They considered the following four geometries of the subsoiler shank and chisel: vertical shank with 31° inclined chisel, vertical shank with 23° inclined chisel, vertical shank with 15° inclined chisel, and 75° rake angle shank with 15° inclined chisel. The soil-tool interface behavior was assumed to be dominated by Coulomb friction (i.e., no adhesion since the dry soil used in the study had negligible adhesion). The model over-predicted force values as compared with values measured in a laboratory soil bin environment for all cases. The over-prediction was 11 to 16.8% for the non-homogenous soil and 15% to 18.4% for the homogenous soil. The subsoiler with a 75° rake angle shank and a 15° inclined angle for chisel required the least amount of draft.

Fielke (1999) investigated the effect of cutting edge geometry of a 400 mm wide experimental sweep on horizontal and vertical components of forces. As well, he studied soil failure patterns, and soil movement below the tillage depth using a 2-D FEM. The results showed that replacing a sharp cutting edge tool with a blunt one can increase draft requirement up to 80%. In addition, the direction of the vertical force can change from one that acts to pull the tool into the soil to a force that provides tool lift. The soil medium was represented by a linear elasto-plastic model, and the Mohr- Coulomb theory was employed as the soil failure criterion. For simplified tillage tool geometries, the finite element model was able to calculate similar draught and vertical forces to those calculated using the Universal Earthmoving Equation. The draught and vertical force calculations for the various cutting edge geometries were found to correlate well with the measured forces from the experimental sweep test.

Plouffe et al. (1999) employed a 3-dimensional FEM to simulate forces applied on a moldboard plow during an operation. The study implemented three plowing depths of 100, 150, and 200 mm and three forward speeds of 0.25, 1, and 2 m/s. A cylindrical plow bottom was fixed on a triaxial dynamometer and its movement in both vertical and lateral directions was controlled by two hydraulic cylinders. The type of soil used in the soil bin was a Sainte-Rosalie clay soil (53% clay, 27% silt, 20% sand, and 2.97% organic matter), which is a typical soil for moldboard plowing in Quebec, Canada. The results showed no significant difference between experimental and simulated data for the

longitudinal forces (F_x). However, the simulated vertical forces (F_z) were significantly lower than measured forces for the forward speeds of 0.25 and 2 m/s. Both experimental and simulated results showed an increase in F_y as depth and speed increased.

2.3. RATIONALE FOR MS RESEARCH

For the past five decades, analytical methods, especially the passive earth pressure theory has predominantly been used to study the soil failure patterns around a cutting tool. The method has been used to develop force prediction models for design optimization. The models developed have been limited in their application because of the underlying assumptions and the over-simplification of the design conditions. In recent years, significant progress has been made with numerical methods, mostly by the finite element method. The finite element method allows the complexity of the geometry and nonlinear stress-strain behavior of the soil-tool interaction to be modeled. However, the success of the FEM in providing accurate and reliable predictions for soil-blade interaction behavior critically hinges on the accuracy and capability of the constitutive models employed in the analysis.

Duncan and Chang's (1970) hyperbolic model has been used extensively for soil-tool interaction modeling (Chi and Kushwaha, 1989; Pollock et al., 1986; Bailey et al., 1984; Yong and Hanna, 1977). The nonlinear elastic formulation was developed for pre-failure behavior. It is a good representation for the stress-strain response for many soils and soft rocks under standard triaxial loading at constant confining stress up to a shear-induced failure. Once shear failure occurs (failure criterion is reached), the hyperbolic model is unable to implement post-failure phenomenon (strain hardening or softening). Rather, the stress path is restricted to the elastic stress space. Duncan (1994) states that simple elasticity models, such as the hyperbolic model, are suitable for stable structures where deformations are small. During the process of soil cutting, the formation undergoes large shear deformations at failure. Therefore, the hyperbolic model is not suitable for collapse load computations (as in the case of excavation or cutting) in the fully plastic range. Potential numerical stability issues may occur when shear failure is approached (Schanz et al., 1999). For accurate predictions of stress-strain behavior of soils near

failure, Duncan (1994) states that more complex elastic-plastic models should be used. Consequently, this research would not employ the hyperbolic model in the finite element model of the soil-blade interaction.

This study is a pioneering effort in the use of the Modified Cam-clay model in soil-blade interaction model. The Modified Cam-clay is an elasto-plastic strain hardening model, capable of modeling the non-linear behavior of soil by means of hardening plasticity. The MCC model is based on the critical state soil mechanics. This model has proven to be accurate in predicting the behavior of soils under quasi-static and monotonic loading conditions (Wroth, 1975; Wood, 1990). Moreover, it is based on few parameters which can be obtained from conventional laboratory tests (Schofield and Wroth, 1968; Atkinson and Bransby, 1978). These aspects make the Modified Cam-clay frequently adopted for research and design purposes in fields involving soils and other materials (Saada et al., 1996; Martin et al., 1997).

Based on this pioneering initiative, the results are expected to provide further insight (evolution of soil failure surface, soil displacement fields and volumetric behavior of soil) into the interaction between a cutting blade and the contact formation. This information will aid industry in the efficient and effective use of excavating machines (bulldozer) for increased productivity and reduced maintenance and total operating costs.

2.4. CRITICAL STATE SOIL MECHANICS

A soil is said to be in critical state when it undergoes large shear deformations at constant volume and constant shear and normal effective stress (Schofield and Wroth, 1968). A locus of critical states of all shear tests on a soil is called a Critical State Line (CSL). The CSL is plotted in a 3-D space consisting of deviatoric stress, mean-normal effective stress and void ratio. Where a particular soil sample will end up on the CSL depends on its initial void ratio, initial mean normal effective stress and the stress path. All the elasto-plastic models, based on the critical state concept, have a well defined yield locus that can be either isotropic or anisotropic. These models are not based on the Mohr-Coulomb failure criterion although the slope of the CSL can be readily correlated with the critical state angle of internal friction.

2.4.1. Elasto-Plastic Soil Constitutive Models. The basic requirement for integrated analyses of deformation and failure of a soil mass is a constitutive relationship. It should be capable of modeling the stress-strain behavior of soil in the elastic and plastic range. Development of such a relationship generally involves separating the elastic and plastic behavior. This is achieved using a well-defined curve known as the yield locus located in a shear stress – normal stress space (Wood, 1990). If the stress state of a soil plots inside the yield locus, it is considered to be elastic and undergoes recoverable deformation. On the other hand, if a particular stress path puts the stress state of the soil on or outside the yield locus, plastic or irrecoverable deformation of soil occurs. Elasto-plastic constitutive models help distinguish between the recoverable and irrecoverable deformations for understanding the stress-strain behavior of soil during loading and unloading.

The constitutive behavior of geomaterials can be effectively modeled in the framework of the elasto-plastic theory. This is because of the main aspects of the mechanical response of geomaterials, such as strong non-linearity, irreversibility, pressure dependence, shear induced contractancy or dilatancy, volumetric hardening and softening. As a matter of fact, the theory of plasticity is adopted for the solution of the simplest and most frequent geotechnical engineering problems. Examples include bearing capacity of foundations, stability of retaining structures and slope stability.

A major aspect of geomaterial mechanical response is the pressure dependence. In the elasto-plasticity framework, this feature can be modeled assuming that the deviatoric section of the yield surface increases with compression. These “conical” yield surfaces were proposed by Drucker and Prager (1952), Drucker (1953) and Shield (1955). However, these classical yield criteria do not predict the development of inelastic strains under isotropic compression (Callari et al., 1998). Furthermore, the assumption of an associative flow rule leads to an overestimation of the dilatant behavior of soils. To overcome the first limitation, a conical yield surface closed by a cap along the hydrostatic axis (Cap-model) was proposed by Drucker et al. (1957). The description of the soil dilatant behavior was improved with the Cam-clay model, developed in Cambridge during the 1960s (Roscoe and Schofield, 1963). This model distinguishes between the yield surface and the surface representing the “ultimate” condition of material. The latter

is a conical surface; it is called “critical” and it represents the soil states characterized by no increments of the volumetric plastic strain.

Most of the large number of elasto-plastic models proposed for clays in the last three decades can be considered as improvements of the Cam-clay (Wroth and Houlsby, 1985; Gens and Potts, 1988). The Modified Cam-clay model (Roscoe and Burland, 1968) differs from the original formulation for the shape of the yield curve. This model has proven to be quite accurate in predicting the behavior of soft clays under quasi-static and monotonic loading conditions (Wroth, 1975; Wood, 1990).

2.4.2. Modified Cam Clay (MCC). The Modified Cam Clay (Roscoe and Burland, 1968) was modified after the original Cam Clay (Roscoe et al. 1958) model. The MCC was proposed on the basis of experimental evidence obtained from axisymmetric shear tests (the so called triaxial tests) on isotropically consolidated remoulded clay samples. The model is capable of describing the stress-strain behavior of soils. It can predict the pressure-dependent soil strength and the compression and dilatancy (volume change) caused by shearing. The MCC model is based on critical state soil mechanics. In critical state mechanics, the state of a soil sample is characterized by three parameters: effective mean stress, deviatoric (shear) stress, and specific volume. Under general stress conditions, the mean stress and the deviatoric stress can be expressed in terms of principal stresses as in Equations (2.4) and (2.5).

$$p' = \frac{1}{3}(\sigma'_1 + \sigma'_2 + \sigma'_3) \tag{2.4}$$

$$q = \sqrt{\left\{\frac{1}{2}[(\sigma'_1 - \sigma'_2)^2 + (\sigma'_2 - \sigma'_3)^2 + (\sigma'_3 - \sigma'_1)^2]\right\}} \tag{2.5}$$

The specific volume is defined in Equation (2.6).

$$v = 1 + e \tag{2.6}$$

2.4.2.1 Normal consolidation line and unloading-reloading lines. The MCC relates the specific volume and $\ln p'$ of a soft soil sample by a straight normal consolidation line (also known as the virgin compression line) and a set of straight swelling lines (Figure 2.4). This relationship is based on the assumption that the soft soil sample is slowly compressed under isotropic stress conditions ($\sigma'_1 = \sigma'_2 = \sigma'_3 = p'$), and under perfectly drained conditions (pore pressure not allowed to build up). The swelling lines are also called unloading-reloading lines.

The loading (normal consolidation) and unloading (swelling) behavior of the MCC model is illustrated in Figure 2.4. When a soil element is first loaded to isotropic stress p'_b, on the plane of $\mathrm{v} - \ln p'$, it moves down the virgin consolidation line from point a to point b. If the sample is unloaded the specific volume–mean stress behavior moves up the swelling line $\overline{bc}$ to point c. If the sample is now reloaded to a stress p'_d, it will first move down the swelling line for stress values up to p'_b. Once p'_b is exceeded, the sample will again move down the virgin consolidation line to the point d. If the sample is then unloaded to a stress value of p'_a, this time it will move up the swelling line $\overline{de}$.

The normal consolidation line in Figure 2.4 is defined by Equation (2.7) as

$$v = N - \lambda ln p' \tag{2.7}$$

while the equation for a swelling line has the form in Equation (2.8).

$$v = v_s - \kappa ln p' \tag{2.8}$$

The values λ, κ and N are characteristic properties of a particular soil.

As can be seen on Figure 2.4, v_s differs for each swelling line, and depends on the loading history of a soil. If the current state of a soil is on the virgin consolidation (normal compression) line, the soil is described as being normally consolidated. If the soil is unloaded as is described by the line $\overline{bc}$, it becomes overconsolidated. In general, soil does not exist outside the virgin consolidation line; when it does that state is unstable.

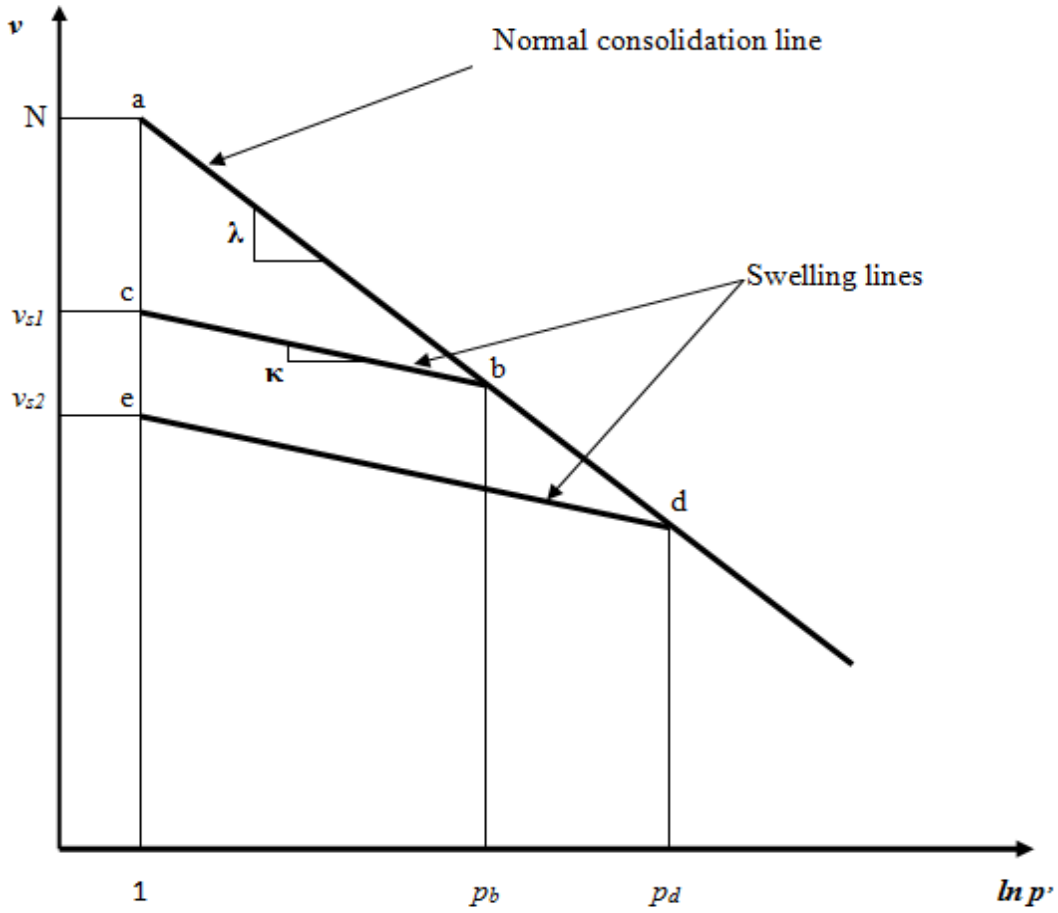

Figure 2.4 Behavior of soil sample under isotropic compression

2.4.2.2 Yielding. The yield locus for the Modified Cam Clay model is defined using an elliptical curve as shown in Figure. 2.5. The position of the yield surface is defined by the preconsolidation pressure, p'_o (a measure of the highest stress level the soil has ever experienced). The parameter M is the slope of the critical state line in the p'-q space. The point C represents the point on the yield curve with horizontal slope. At this point plastic volumetric strain is zero and the yield surface becomes stationary. A point like C is the final state for a soil taken to failure, independently of initial conditions. This state is called critical state. If a soil element yields at a point to the right of C (wet or subcritical side), plastic volumetric strains are positive and hardening is ensured. If yielding takes place to the left of C (dry or supercritical side), plastic volumetric strains are negative and softening is resulted.

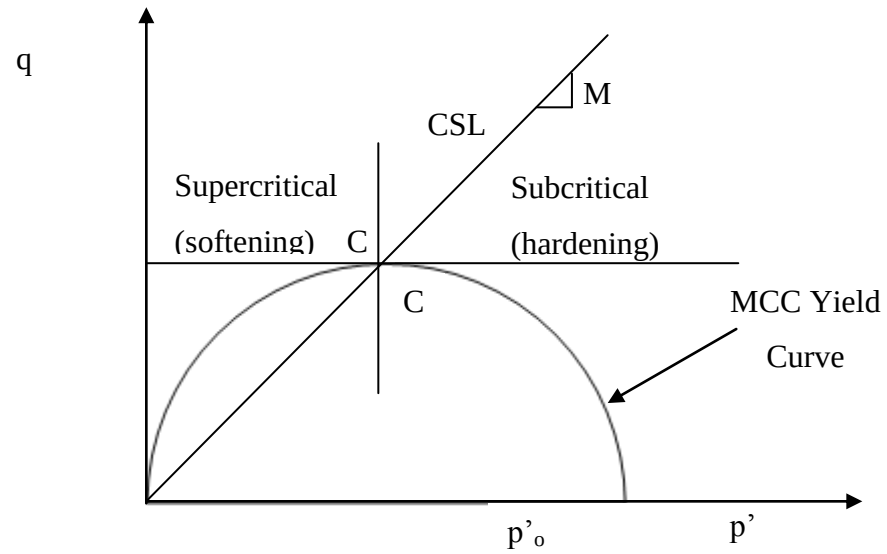

Figure 2.5 Yielding for the Modified Cam Clay Model

2.5. SUMMARY

An extensive literature survey has been carried out by reviewing the relevant literature to evaluate the contributions and limitations of the current body of knowledge on cutting tool-formation interaction. The literature was also used to establish the frontier in this research domain.

Analytical methods have been used over the last five decades to develop force predictive models for soil cutting/excavation. Osman (1956) was the first to use the passive earth pressure theory to study the mechanics of 2D soil cutting blades. Reece (1965), proposed the universal earthmoving equation (UEE) for describing the force necessary to cut soil with a tool using the grouping of Osman (1964). Swick and Perumpral (1988) modified the 3D model developed by Perumpral et al. (1983) to account for the dynamic effect. The analytical models have been successful to some extent. However, the methodology for developing these models has intrinsic weaknesses that limit their application.

Numerical methods have gained popularity in machine-formation interaction in recent decades. The discrete element method and the finite element method are the two

numerical methods applied to study the interaction between a cutting tool and soil. The existing applications of the DEM have concentrated on attempts to model soil samples in a container (Tanaka et al., 2000) and as a block of soil (Momozu et al., 2003). Given the large numbers of particles during excavation, the current state of the DEM techniques seems incapable of solving these problems even with the resolution of the force predictions (Awuah-Offei, 2005). The finite element method has been used in recent decades to model the interaction between a cutting blade and soil. Yong and Hanna (1977) were the first to apply the FEM in a 2D soil failure model. Chi and Kushwaha (1991) improved on the model by developing a 3D nonlinear model. The dynamic interaction between soil and tillage tool was investigated by Kushwaha and Shen (1995) using a 2D finite element analysis.

This chapter also critiques the constitutive models used in FEM analysis of soil tool interaction. Duncan and Chang's (1970) hyperbolic model has been used extensively to describe the mechanical behavior of soil and at the soil-tool interface (Chi and Kushwaha, 1989; Pollock et al., 1986; Bailey et al., 1984; Yong and Hanna, 1977). The advantage of the hyperbolic model is its simplicity. However, the model is unable to implement post-failure phenomenon once shear failure occurs. This may lead to potential numerical instability. The constitutive behavior of geomaterials can be effectively modeled in the framework of the elasto-plastic theory. The Drucker-Prager's (1952) elastic-perfectly plastic model has been used (Araya and Gao, 1995; Davoudi et al., 2008) in cutting tool formation interaction. The model is incapable of predicting the plastic volumetric strain of soil, which may lead to the underestimation of the peak shearing resistance of the soil. The soil constitutive equations used in the available FE models fail to adequately capture the elastic and plastic behaviors of soil formations. The Modified Cam Clay model is an elasto-plastic model based on the critical state soil mechanics. The model has proven to be accurate in predicting the behavior of soils under quasi-static and monotonic loading conditions (Wroth, 1975; Wood, 1990). This research initiative advances the frontiers in formation failure mechanics and machine-formation interactions by using appropriate elasto-plastic constitutive model of the soil formation.

3. MATERIAL AND NUMERICAL MODELING

Chapter 3 deals with the numerical modeling framework for achieving the research objectives. The chapter presents the constitutive relation between incremental stress and strain of the Modified Cam-clay model. FEM formulation is used to derive the element stiffness equations of the soil-blade interaction problem. Also presented are the numerical solution and convergence of the nonlinear finite element equations. The chapter thoroughly discusses the computer simulation environment and its features in the context of soil-blade interaction modeling. The experimental design and experimentation process adopted for the soil blade interaction are also contained in this chapter.

3.1. MODIFIED CAM-CLAY MODEL (ROSCOE AND BURLAND, 1968)

The Modified Cam-clay is an elasto-plastic strain hardening model, capable of modeling the non-linear behavior of soil by means of hardening plasticity. The MCC model is based on the critical state soil mechanics described in Section 2.3. A soil is said to be in critical state when it undergoes large shear deformations at constant volume, and constant shear, and normal effective stress. The objective of a soil constitutive model is to develop explicit relations of incremental stress and strain equations. In the MCC model, the total strain increments (volumetric and shear strains), caused by stress increments (mean and deviatoric stresses), are divided into an elastic component and a plastic (irrecoverable) component as expressed in Equations (3.1) and (3.2).

$$d\varepsilon_v = d\varepsilon_v^e + d\varepsilon_v^p \tag{3.1}$$

$$d\varepsilon_s = d\varepsilon_s^e + d\varepsilon_s^p \tag{3.2}$$

The general elements of elastoplastic material models for geomaterials can be concluded as: elasticity, yield surface, plastic flow rule, and the hardening-softening evolution laws.

3.1.1. Elasticity. Based on Hooke's elastic law, the incremental stress is proportional to incremental strains equation as shown in Equation (3.3).

$$\begin{Bmatrix} dq \\ dp' \end{Bmatrix} = \begin{bmatrix} 3G & 0 \\ 0 & K' \end{bmatrix} \begin{Bmatrix} d\varepsilon_s^e \\ d\varepsilon_v^e \end{Bmatrix} \tag{3.3}$$

The bulk modulus is not constant. It depends on the mean stress, specific volume and slope of the swelling line, and is calculated by Equation (3.4)

$$K = \frac{vp'}{\kappa} \tag{3.4}$$

The Modified Cam-Clay formulation requires specification of either shear modulus or Poisson's ratio. When G is given as a constant then μ is no longer a constant, and is calculated from Equation (3.5).

$$\mu = \frac{3K-2G}{2G+6K} \tag{3.5}$$

Similarly, when μ is given as a constant then G is determined using Equation (3.6).

$$G = \frac{3(1-2\mu)}{2(1+\mu)} K \tag{3.6}$$

3.1.2. Yield Surface Function. Equation (3.7) expresses a typical form of the yield function.

$$f(\sigma, q_*) = 0 \tag{3.7}$$

The stress state inside the yield surface is assumed to be elastic. When a stress state satisfies the yield surface function, plastic deformation takes place. The yield function for the MCC model is defined in Equation (3.8).

$$f = \frac{q^2}{p'^2} + M^2\left(1 - \frac{p'_o}{p'}\right) = 0 \tag{3.8}$$

The parameter p'_o controls the size of the yield surface and is different for each unloading-relaoding line. It is used to define the hardening behavior of soil.

3.1.3. Plastic Flow Rule. The direction of elastic strain increment generally coincides with the direction of the stress increment. The direction of plastic strain increment is usually not coaxial with the direction of the stress increment, and its magnitude is not as easily determined as that of elastic strain. Therefore, a flow rule is proposed to determine the direction and relative magnitude of plastic strain increment after the yield surface is contacted. The plastic flow directions are usually derived from potential function. If potential function is assumed to be the same as yield function, it is called associated flow rule. If potential function is different from yield function, it is called non-associated flow rule. The associated flow rule is assumed in the MCC model. Equations (3.9) and (3.10) define the generalized flow rule for shear and volumetric plastic strains respectively.

$$d\varepsilon_s^p = d\Lambda\frac{\partial f}{\partial q} \tag{3.9}$$

$$d\varepsilon_v^p = d\Lambda\frac{\partial f}{\partial p'} \tag{3.10}$$

3.1.4. Hardening-Softening Evolution Laws. When a soil undergoes shearing, it behaves elastically until it hits the initial yield surface. From then on, the yield surface begins to expand/contract and exhibits hardening/softening behavior. The change in size and/or shape of yield surface and potential surface is controlled by hardening-softening evolution laws. Hardening/softening for the MCC is isotropic and is controlled by the parameter p'_o, which is related to the plastic volumetric strain. The volumetric hardening law is expressed in rate form as shown in Equation (3.11)

$$d\varepsilon_v^p = \frac{(\lambda - \kappa)}{(1+e_o)}\frac{dp'_o}{p'_o} \tag{3.11}$$

The plastic volumetric and shear strain increments for the MCC model are given by Equations (12) and (13) respectively.

$$d\varepsilon_v^p = \frac{\lambda-\kappa}{1+e}\left(\frac{dp'}{p'}+\frac{2\eta\, d\eta}{M^2+\eta^2}\right) \tag{3.12}$$

$$d\varepsilon_s^p = \frac{\lambda-\kappa}{1+e}\left(\frac{dp'}{p'}+\frac{2\eta\, d\eta}{M^2+\eta^2}\right)\frac{2\eta}{M^2-\eta^2} \tag{3.13}$$

The parameter η is defined in Equation (3.14).

$$\eta = \frac{q}{p'} \tag{3.14}$$

3.2. FINITE ELEMENT MODELING

3.2.1. FEM Formulation. The schematic representation of the FEM formulation stages is illustrated in Figure 3.1. In many applications, it is possible to approximate a 3D problem to a simpler 2D application in which only the x-y plane is modeled. The plain strain condition deals with a situation in which the dimension of the structure in one direction (example the z-direction) is very large in comparison with the dimensions in the other two directions. In such a case, the applied forces act in the x-y plane and do not vary in the z-direction. Dozer blades used in surface mining applications have widths significantly greater than the cutting depth. Hence, this finite element model is simplified to a 2D plain strain problem. The first step in the FEM formulation is to divide the structure into elements and examine the behavior of a typical element. Solid (or continuum) elements are mostly used for linear analysis and complex nonlinear analyses involving contact, plasticity, and large deformations. (Becker, 2004). The soil-tool interaction process involves permanent deformation and large displacements of the formation. Hence, continuum elements will be used in the FE formulation of the soil-cutting blade interaction process. In continuum elements, the degrees of freedom are the displacement components. The shape functions of an element are defined by assuming linear, quadratic or higher-order interpolation functions for the displacements. A linear

shape function was used with 4-node (quadrilateral) continuum elements for simplicity and numerical efficiency. This means that the displacement is allowed to vary linearly per element, and the stress/strain is constant per element. The basic strategy for FE formulations is to treat the nodal displacements as the unknown or independent variables to be determined by solving a system of linear algebraic equations. The displacement functions are differentiated to obtain the strains, and the constitutive (stress-strain relations) equations are used to satisfy the material law. After generating the strain equations, an element stiffness matrix is derived by using either a direct equilibrium of forces approach or a more general energy approach. All contributions from the individual elements are added together to form the overall stiffness matrix, which is a sparsely populated matrix.

Boundary conditions and external loads are applied to satisfy the prescribed displacement and applied force conditions. The system of linear algebraic equation is solved to obtain the nodal displacements. Forces, strains, and stresses are obtained from the computed displacements by using stress-strain displacement relationships. The strains are obtained by differentiating the displacements over each element. The stresses are derived from the strains using the material law (the constitutive equations).

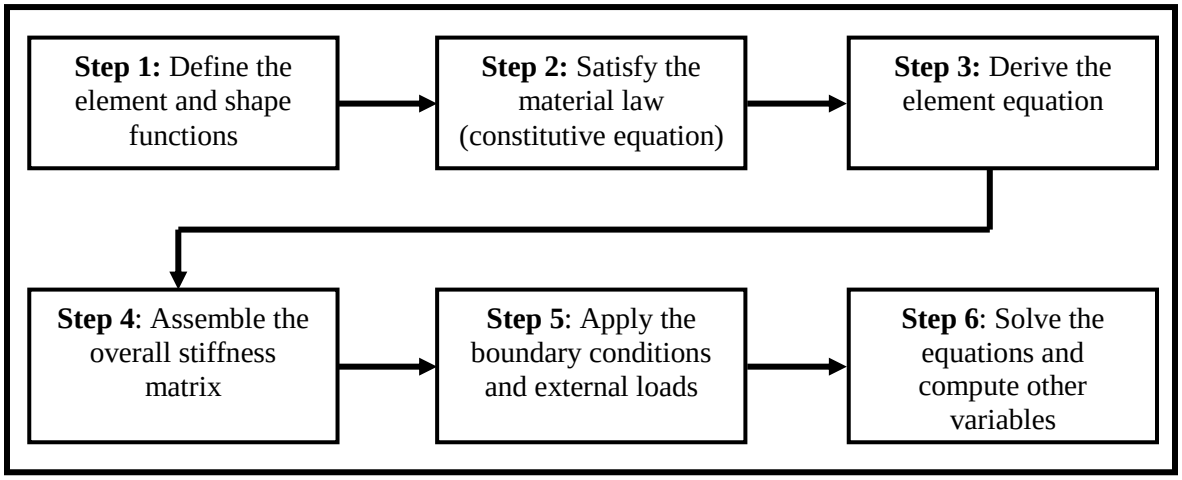

Figure 3.1 The stages in the FEM formulation

The variables used in the 2D FE formulation are defined in Equations (3.15), (3.16) and (3.17). In 2D continuum problems, the variables are displacements, strains and stresses.

$$[u] = \begin{bmatrix} u_x \\ u_y \end{bmatrix} \tag{3.15}$$

$$[\varepsilon] = \begin{bmatrix} \varepsilon_{xx} \\ \varepsilon_{yy} \\ \varepsilon_{xy} \end{bmatrix} \tag{3.16}$$

$$[\sigma] = \begin{bmatrix} \sigma_{xx} \\ \sigma_{yy} \\ \sigma_{xy} \end{bmatrix} \tag{3.17}$$

Assuming a linear variation of displacement over each quadrilateral element, an expression for the displacement in terms of x and y can be written as shown in Equations (3.18) and (3.19).

$$u_x(x,y) = N_1(x,y)u_{x1} + N_2(x,y)u_{x2} + N_3(x,y)u_{x3} + N_4(x,y)u_{x4} \tag{3.18}$$

$$u_y(x,y) = N_1(x,y)u_{y1} + N_2(x,y)u_{y2} + N_3(x,y)u_{y3} + N_4(x,y)u_{y4} \tag{3.19}$$

Equation (3.20) expresses the displacement functions in a matrix form.

$$u_i(x,y) = [N]^T[u_e] \tag{3.20}$$

$$[N] = \begin{bmatrix} N_1 \\ N_2 \\ N_3 \\ N_4 \end{bmatrix} \tag{3.21}$$

Using the strain-displacement definitions, the element strain can be determined by differentiating Equations (3.18) and (3.19).

$$\varepsilon_{xx} = \frac{\partial u_x}{\partial x} = \frac{\partial N_1}{\partial x}u_{x1} + \frac{\partial N_2}{\partial x}u_{x2} + \frac{\partial N_3}{\partial x}u_{x3} + \frac{\partial N_4}{\partial x}u_{x4} \tag{3.22}$$

$$\varepsilon_{yy} = \frac{\partial u_y}{\partial y} = \frac{\partial N_1}{\partial y}u_{y1} + \frac{\partial N_2}{\partial y}u_{y2} + \frac{\partial N_3}{\partial y}u_{y3} + \frac{\partial N_4}{\partial y}u_{y4} \tag{3.23}$$

$$\varepsilon_{xy} = \frac{\partial u_x}{\partial y} + \frac{\partial u_y}{\partial x} = \frac{\partial N_1}{\partial y} u_{x1} + \frac{\partial N_2}{\partial y} u_{x2} + \frac{\partial N_3}{\partial y} u_{x3} + \frac{\partial N_4}{\partial y} u_{x4} + \frac{\partial N_1}{\partial x} u_{y1} + \frac{\partial N_2}{\partial x} u_{y2} + \frac{\partial N_3}{\partial x} u_{y3} + \frac{\partial N_4}{\partial x} u_{y4} \quad (3.24)$$

The element strain vector $[\varepsilon_e]$ can then be written in matrix form as shown in Equation (3.25).

$$[\varepsilon] = \begin{bmatrix} \varepsilon_{xx} \\ \varepsilon_{yy} \\ \varepsilon_{xy} \end{bmatrix} = \begin{bmatrix} \frac{\partial N_1}{\partial x} & 0 & \frac{\partial N_2}{\partial x} & 0 & \frac{\partial N_3}{\partial x} & 0 & \frac{\partial N_4}{\partial x} & 0 \\ 0 & \frac{\partial N_1}{\partial y} & 0 & \frac{\partial N_2}{\partial y} & 0 & \frac{\partial N_3}{\partial y} & 0 & \frac{\partial N_4}{\partial y} \\ \frac{\partial N_1}{\partial y} & \frac{\partial N_1}{\partial x} & \frac{\partial N_2}{\partial y} & \frac{\partial N_2}{\partial x} & \frac{\partial N_3}{\partial y} & \frac{\partial N_3}{\partial x} & \frac{\partial N_4}{\partial y} & \frac{\partial N_4}{\partial x} \end{bmatrix} \begin{bmatrix} u_{x1} \\ u_{y1} \\ u_{x2} \\ u_{y2} \\ u_{x3} \\ u_{y3} \\ u_{x4} \\ u_{y4} \end{bmatrix} \quad (3.25)$$

or, more concisely as expressed in Equation (3.26).

$$[\varepsilon] = [B][u_e] \quad (3.26)$$

The elasto-plastic constitutive stress strain law (MCC) of a soil can be expressed incrementally as shown in Equation (3.27). $[D^{ep}]$ is an elasto-plastic matrix which is a function of the current stress level but independent of the increments of stress and strain.

$$[\Delta\sigma] = [D^{ep}][\Delta\varepsilon] \quad (3.27)$$

Using an energy formulation to derive the stiffness matrix is more robust than the procedure adopted by using equilibrium conditions. This is because the energy formulation also applies to other types of elements (such as quadratic or cubic elements) and to 3D problems (Becker, 2004). The total potential energy (Π) of the element, expressed in Equation (3.28) is the difference between the strain energy and the work done by the external forces (blade cutting forces).

$$\Pi = \int_V \frac{1}{2}[\sigma]^T[\varepsilon]dV - [u_e]^T[F_e] \tag{3.28}$$

where v is the volume of the element. Susbstituting Equations (3.26) and (3.27) into Equation (3.28) results in Equation (3.29).

$$\Pi = \int_V \frac{1}{2}[u_e]^T[B]^T[D^{ep}][B][u_e]dV - [u_e]^T[F_e] \tag{3.29}$$

The principle of minimum total potential energy states that when a body is in equilibrium, the value of Π must be stationary with respect to the variables of the problem. The equilibrium is stable if the total potential energy is minimum (and unstable if it is maximum). In most FE formulations, the displacement is chosen as the unknown/independent variable of the problem (Becker, 2004). Using the principle of minimum total potential energy, the differential of the total potential energy with respect to the displacement must be zero (Equation (3.30)). The minimum potential energy is given by Equation (3.31).

$$\frac{\partial \Pi}{\partial [u_e]} = 0 \tag{3.30}$$

$$\int_V [B]^T[D^{ep}][B][u_e]dV - [F_e] = 0 \tag{3.31}$$

Equation (3.32) expresses the minimum potential energy equation in terms of the element stiffness matrix, $[K_e]$.

$$[K_e][u_e] = [F_e] \tag{3.32}$$

The element stiffness matrix in Equation (3.32) is defined in Equation (3.33).

$$K_e = \int_V [B]^T [D^{ep}][B] dV \tag{3.33}$$

To form the overall stiffness matrix, all the energy contributions from the individual elements are added together, as shown in Equation (3.34).

$$\left(\frac{\partial \Pi}{\partial [u_e]}\right)_{overall} = \sum_{All\ elements} \left(\frac{\partial \Pi}{\partial [u_e]}\right)_{element} = 0 \tag{3.34}$$

The overall stiffness matrix equation assumes that element interfaces do not contribute to the overall energy of the structure. The final global system of equations is expressed in Equation (3.35). Boundary conditions are imposed on the assembled element equations and solved using an iterative solution technique.

$$[K]_{global}[U]_{global} = [F]_{global} \tag{3.35}$$

3.2.2. Numerical Solution. The finite element equation as given by Equation (3.35) is a nonlinear equation because the strain displacement matrices and the constitutive matrix are functions of the displacement. A geometric and material nonlinear finite element is most effectively performed using an incremental formulation. The static variable is updated incrementally corresponding to successive load steps (or time steps in dynamics) in order to trace out the complete solution path (Bathe et al., 1973; Bathe et al., 1978). In this solution, it is important that the governing finite element equations are satisfied in each load step to sufficient accuracy. There are several iterative schemes adopted to solve the nonlinear equations in Equation (3.35). The most frequently used iteration schemes are some form of Newton-Raphson iteration (Bathe and Cimento, 1979). The Newton-Raphson method has fast convergence and the number of iterations required for convergence is usually smaller than other methods. The overall performance of this approach is usually better (lesser solution time) than with other iterative methods. Equation (3.36) constitutes the Newton-Raphson solution of the nonlinear finite element equation. The superscripts denote the number of iterations.

$$\widehat{K}^{(i-1)}\Delta U^{(i)} = F - R(U^{(i-1)}) \quad (3.36)$$

$$\Delta U^{(i)} = U^{(i)} - U^{(i-1)} \quad (3.37)$$

$$\widehat{K}^{(i-1)} = \left(\frac{d\Psi}{dU}\right) \quad (3.38)$$

$$\Psi(U) = K(U)U - F \quad (3.39)$$

The iteration using Equation (3.36) continues until appropriate termination criteria are satisfied. If an incremental solution strategy based on iterative methods is to be effective, realistic criteria should be used for the termination of the iteration. At the end of each iteration, the solution obtained is checked to see whether it has converged within preset tolerances or whether the iteration is diverging. A more reliable convergence criterion is based on the out-of-balance forces (Bathe and Cimento, 1979). A force convergence criterion requires that the norm of the out-of-balance load vector be within a preset tolerance limit of the original load increment.

3.3. FINITE ELEMENT IMPLEMENTATION

A capability review of the available finite element codes was carried out by Aboelnor (2002) to assess the most appropriate code for simulating the soil-tool interaction problem. The following commercial finite element codes were considered: ABAQUS (HKS, Hibbit 2000), ANSYS, DYNA, and open source codes such as TOCHNOG. The study concluded that ABAQUS was the most appropriate for the following reasons:

1. A wide range of element types, including continuum elements (1d, 2d, 3d), beams, membranes and shells.
2. Element formulations are suitable for large displacements rotations and strains; implemented within an updated Lagrangian framework.
3. Conventional material models for metals, soil, clay, concrete, jointed rock, plastics and rubber are available. The Modified Cam Clay soil model is included in the material models library.
4. User-defined subroutine (UMAT) permits inclusion of additional material models. This feature is not included in ANSYS.

5. Surface-to-surface contact with frictional sliding.
6. Extensive documentation, including a Theory Manual, User's Manual (3 volumes), Example Problems Manual (2 volumes) and Verification Manual.

In addition to the capabilities/features indicated above, Abaqus' availability was critical to its selection for this analysis.

A complete finite element analysis in Abaqus usually consists of three distinct stages: preprocessing, simulation, and post-processing. These three stages are linked together as shown in Figure 3.2.

1. Preprocessing: In this stage, the model of the physical problem is defined in order to create an Abaqus input file. The model is usually created graphically using Abaqus/CAE or another preprocessor. Altair Hyperworks (Hypermesh) was used in this work instead of Abaqus/CAE for the preprocessing. Altair HyperMesh is a high-performance finite element pre-processor that provides a highly interactive and visual environment to analyze product design performance. It's highly flexible and provides much greater user control on creating model geometry and meshing. It is also compatible with Abaqus. In order to perform finite element analysis, it is required to generate a valid finite element mesh. The created model meets this validity with the following characteristics: (i) adjacent regions of geometry share matching boundaries and vertices; (ii) the geometric components form a closed surface or solid region; (iii) there is no overlap between adjacent regions.

In order to obtain a unique solution of the problem, some constraints or boundary conditions and loading conditions must be prescribed at some of the nodes. The boundary and loading conditions may represent displacement and/or force conditions.

2. Simulation (Abaqus/Standard or Abaqus/Explicit): The simulation, which normally is run as a background process, is the stage in which Abaqus/Standard or Abaqus/Explicit solves the numerical problem defined in the model. The input file generated by the pre-processor is used to construct the element stiffness matrices of each element. The element stiffness matrices are assembled to form the overall system of simultaneous equations. Abaqus/Standard uses Newton's method to solve the nonlinear equilibrium

equations. The MCC problem involves history-dependent response; therefore, the solution usually is obtained as a series of increments, with iterations to obtain equilibrium within each increment. Increments must be kept small (in the sense that rotation and strain increments must be small) to ensure correct modeling of history dependent effects. The choice of increment size is a matter of computational efficiency. Too large increments will require more iteration. Furthermore, Newton's method has a finite radius of convergence.

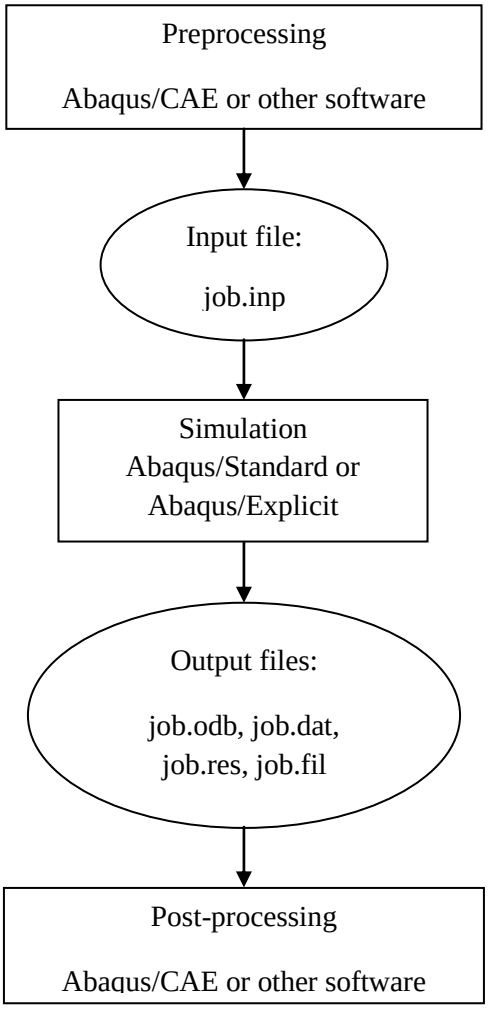

Figure 3.2 A complete FE analysis in Abaqus

Very large increments can prevent solution from being obtained because the initial state is too far away from the equilibrium. Thus, there is an algorithmic restriction on the increment size. Abaqus/Standard automatically adjusts the size of the time increments to solve nonlinear problems efficiently. Nonlinear static problems can be unstable. Such instabilities may be of a geometrical nature, such as buckling, or of a material nature, such as material softening. Abaqus/Standard provides an automatic mechanism for stabilizing unstable quasi-static problems through the automatic addition of volume-proportional damping to the model.

After a successful run, the solver produces an output file which contains all relevant information.

3. Postprocessing: The results can be evaluated once the simulation has been completed and the displacements, stresses, or other fundamental variables have been calculated. The evaluation was done interactively using the Visualization module of Abaqus/CAE.

3.3.1. Abaqus Modeling Features. ABAQUS is a general-purpose finite element program designed specifically for advanced analysis applications (ABAQUS, 2010). A wide variety of problems can be addressed with the available modeling tools. This section highlights features that are required for the analysis of soil-tool interaction in 2D.

3.3.1.1 Analysis type. ABAQUS/Standard provides a variety of time- and frequency-domain analysis procedures. Static stress-displacement analysis was used for all the analysis (Abo-Elnor, 2002). It is usually used when the model can neglect the inertia effects and time-dependent material effects (creep, swelling, and viscoelasticity) and still preserve the system integrity. It is used for equilibrium problems and can include linear or nonlinear response. The effect of such non-linearity can be introduced in a general ABAQUS analysis step.

3.3.1.2 Surface definition. Surfaces, required for the model definition must be defined at the beginning of the simulation. Surface definitions describe the surface of bodies that acontact between two bodies. ABAQUS has three classifications of contact surfaces: (i) Element-based surface; (ii) Node-based surface, and; (iii) Analytical rigid surface.

For 2D analysis of soil-tool interaction, the blade is simulated as an analytical rigid surface using the *RIGID BODY, ANALYTICAL SURFACE option in ABAQUS. The soil surface is simulated using an element-based surface for ease of convergence and reliable results.

A reference point is assigned to the rigid surface or body (blade), through which its motion is described. This feature enables accounting for reaction forces acting on the blade in the soil-tool interaction analysis.

3.3.1.3 Contact modeling. There are two methods for modeling contact and interaction problems in ABAQUS: using surfaces or using contact elements. According to Alboenor (2002), most contact problems are modeled by using surface-based contact, such as the contact between a rigid surface and a deformable body (as in the soil-tool interaction problem). The structures can be either 2- or 3D, and they can undergo either small sliding (sliding distance does not exceed half of the element length) or finite sliding (no limit on the sliding distance so long as the two contact surfaces are in contact).
There are three steps in defining a contact simulation:

1. Defining the surfaces of the bodies that could potentially be in contact,
2. Specifying which surfaces interact with one another (contact pairs), and
3. Defining the mechanical surface interaction model that governs the behavior of the surfaces when they are in contact.

ABAQUS defines contact between two bodies in terms of two surfaces that may interact; these surfaces are called a “contact pair”. The order in which the two surfaces are specified on the *CONTACT PAIR option is critical because of the manner in which surface interactions are discretized. For each node on the first surface (the “slave” surface), ABAQUS attempts to find the closest point on the second surface (the "master" surface) of the contact pair where the master surface's normal passes through the node on

the slave surface. The interaction is then discretized between the point on the master surface and the slave node.

3.3.1.4 Mechanical surface interaction models. Some of the mechanical surface interaction models available in ABAQUS/Standard include:

1. Friction model: When surfaces are in contact, they usually transmit shear as well as normal forces across their interface. Thus, the analysis may need to take frictional forces, which resist the relative sliding of the surfaces, into account. Coulomb friction is a common friction model used to describe the interaction of contacting surfaces. The model characterizes the frictional behavior between the surfaces using a coefficient of friction. The contacting surfaces will not slip (slide relative to each other) until the shear stress across their interface equals the limiting frictional shear stress, which is a function of the normal contact pressure.
2. Finite sliding (relative surface motions): Separation and sliding of finite amplitude and arbitrary rotation of the surfaces may arise. The finite-sliding rigid contact capability is implemented by means of a family of contact elements that ABAQUS automatically generates based on the data associated with the *CONTACT PAIR option. At each integration point, these elements construct a measure of overclosure (penetration of the point on the surface of the deforming body into the rigid surface) and measures of relative shear sliding.
3. Softened contact (interaction normal to the surface): The contact pressure is an exponential function of the clearance between the surfaces.

   To avoid convergence problems in the analysis of soil-tool interaction, mainly when the cut soil separated from the rest of soil bulk, an exponential pressure-overclosure relationship was included using the *SURFACE BEHAVIOR option.

3.3.1.5 Element type. Choosing the appropriate element type for an analysis is one of the most important steps towards a correct simulation and analysis. Element choice is based on the following well established factors:

1. Analysis type: static or dynamic.
2. Material behavior: linear or non-linear.
3. Contact interaction status: whether there is a contact or not.
4. Thickness of structure.
5. Expected degree of distortion of elements.
6. Results needed from the analysis.
7. Analysis dimension, 2D or 3D.

Considering these factors, an element has to be selected according to the main element features in Section 3.3.1.5.1.

3.3.1.5.1 Element family. One of the major distinctions between different element families is the geometry type that each family assumes. Different element family classification is listed below.

1. Continuum solid elements
2. Shell elements
3. Beam elements
4. Rigid elements
5. Membrane elements
6. Infinite elements
7. Connector elements
8. Truss elements

The solid (or continuum) elements in ABAQUS can be used for linear analysis and for complex nonlinear analyses involving contact, plasticity, and large deformations and hence it will be used throughout the soil-tool interaction analysis.

3.3.1.5.2 Number of nodes and order of interpolation. Displacements and/or other degrees-of-freedom are calculated at the nodes of the element. At any other point in the element, the displacements are obtained by interpolating the nodal displacements. Usually the interpolation order is determined by the number of nodes used in the element.

Elements that have nodes only at their corners use linear interpolation in each direction and are often called linear elements or first-order elements. Elements with mid side nodes use quadratic interpolation and are often called quadratic elements or second-order elements.

First order elements are more suitable for analyzing problems where contact exists or nonlinearity and severe element distortion are expected during the analysis. They are also easier to be meshed using automatic mesh generation.

3.3.1.5.3 Element integration. When forming element stiffness, the element may integrate in full mode or reduced mode. When a reduced integration element is used, integration will not be carried out at every element node. Reduced integration reduces running time, especially in three dimensions. In addition, reduced integration is usually recommended for problems involving material nonlinearities such as plasticity and creep problems (Becker, 2004).

3.3.1.5.4 Element dimension. The ABAQUS element library contains elements for modeling a wide range of spatial dimensionality. In this study of soil-tool interaction, the plane strain element was used. Plane strain elements can be used when it can be assumed that the strains in a loaded body or domain are functions of planar coordinates alone and the out-of-plane normal and shear strains are equal to zero. This modeling assumption is generally used for bodies that are very thick relative to their lateral dimensions, such as shafts, concrete dams, or walls. Plane strain theory can be applied for the analysis of soil tool interaction in 2D.

3.3.1.5.5 Summary of recommendations for element usage. The soil-tool interaction model contains contact between the cutting tool and the soil. The soil elements are expected to distort due to the large deformation caused by monotonic

loading during cutting. Hence a 4-node linear integration plane strain continuum element (CPE4) will be used to model the soil in the 2D analysis. ABAQUS will automatically generate the appropriate interface elements for the contact according to the contact topology.

3.3.1.6 Prescribed conditions. The following types of external conditions can be prescribed in an ABAQUS model:

1. Initial conditions: Nonzero initial conditions can be defined for many variables.The initial void ratio and initial stress state of the simulated soil described by the MCC model is specified as an initial condition using the *INITIAL CONDITION option.
2. Boundary conditions: Boundary conditions are used to prescribe values of basic solution variables: displacements and rotations in stress/displacement analysis. During the analysis of the soil-tool interaction, tool displacement is described using the *BOUNDARY option.

3.3.1.7 Linear and nonlinear analysis. A general analysis step is provided by ABAQUS, which can be used to analyze linear or nonlinear response. Non-linearity can be introduced in the model during the step analysis as a consequence of material nonlinearity or/and geometric nonlinearity. Material nonlinearity is accounted for by way of constitutive model integration, but geometry nonlinearity is accounted for by including the NLGEOM parameter in the *STEP option. For the expected large deformation of the cut soil in soil-tool interaction analysis, model nonlinearity was considered.

3.3.1.8 Matrix storage and solution scheme. ABAQUS generally uses Newton's method to solve nonlinear problems and the stiffness method to solve linear problems (Potts and Zdravkovic, 1999). In both cases the stiffness matrix is needed. In some problems, such in Coulomb friction and contact interaction, this matrix is not symmetric.

The nonlinear soil-cutting blade problem was solved with Newton’s method and the unsymmetric matrix storage parameter was used to deal with the contact.

3.3.1.9 Stabilization of unstable problems. Some static problems can be naturally unstable, for a variety of reasons. Instability may occur because unconstrained rigid body motions exist. ABAQUS may be able to handle this type of problem with the *CONTACT CONTROLS, APPROACH option when rigid body motions exist during the approach of two bodies that will eventually come into contact.

Geometrically nonlinear static problems sometimes involve buckling or collapse behavior, where the load-displacement response shows a negative stiffness and the structure must release strain energy to remain in equilibrium. Several approaches are possible for modeling such behavior. One is to treat the buckling response dynamically, thus actually modeling the response with inertia effects included as the structure snaps. Another approach would be to use dashpots to stabilize the structure during a static analysis. ABAQUS offers an automated version of this approach by using the STABILIZE parameter on the static analysis procedures.

For soil-tool interaction analysis, where a geometric nonlinearity of the soil and the rigid body motion of the cutting tool are to be considered, the STABILIZE parameter was included into ABAQUS *STATIC option to avoid convergence problems.

3.4. EXPERIMENTAL DESIGN AND EXPERIMENTATION

The experimental design of the interaction between the soil and the cutting blade in ABAQUS is described. The model geometry, material constitutive model and parameters, boundary and initial conditions of the model. The validation process of the model and the type of experiments conducted to study the soil-cutting blade interaction process are also presented.

3.4.1. Material. The Modified Cam-Clay (MCC) model was used to describe the mechanical behavior of the soil during the cutting process. The plasticity model is available in ABAQUS. Table 3.1 represents the MCC model parameters of the clayey soil used in the finite element modeling.

Table 3.1 MCC parameters for clayey soil (Source: Helwany, 2007)

e	v	k	λ	M	a_o (kPa)
0.889	0.3	0.026	0.174	1	103.35

3.4.2. Model Geometry. The soil block has a width of 2000 mm and a depth of 600 mm. The operating depth and the cutting angle of the blade varied in the analysis. The geometry and dimensions of the soil-blade interface model are shown in Figure 3.3.

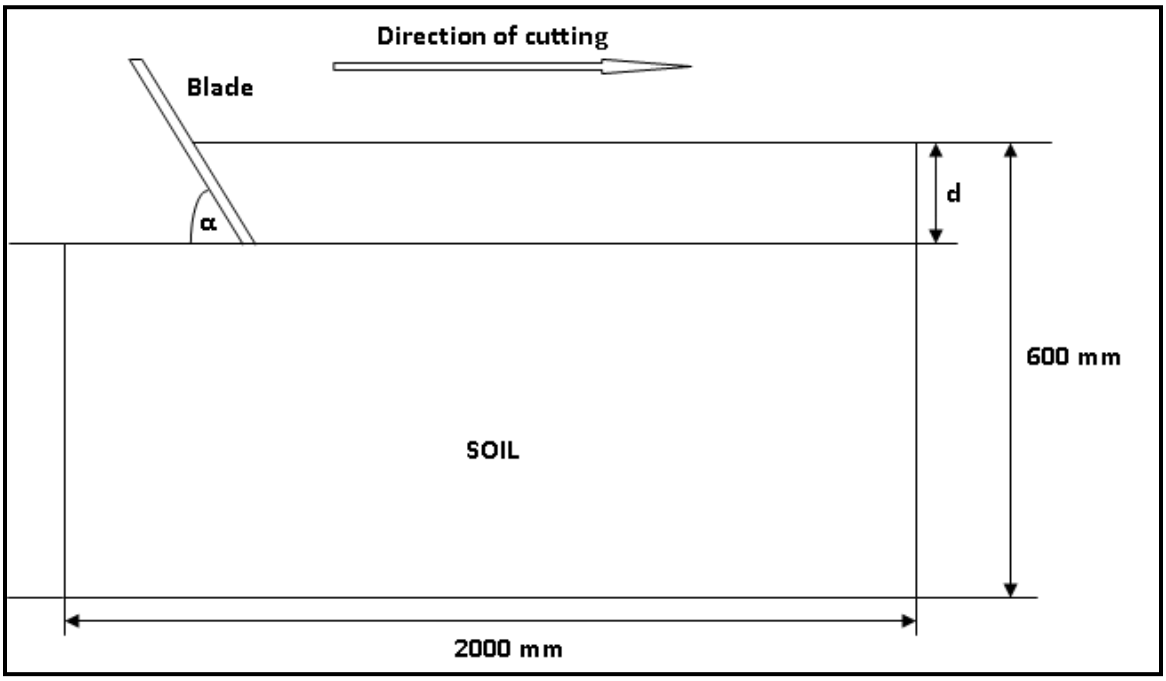

Figure 3.3 Model geometry with dimensions

3.4.3. Meshing and Boundary Conditions. The meshing was performed using the automatic mesh generator of Hypermesh (Altair Hyperworks, 2009) for input to ABAQUS/Standard solver. From the discussion in Section 3.3.1.5, a plane strain 2D bilinear continuum element was used to represent the clayey soil in the finite element model. The number of elements used to simulate the soil and the cutting blade varied,

depending on cutting depth and rake angle of the blade. The blade was defined as a rigid body with a reference node. Motion of the blade is governed by prescribed displacement at the reference node attached to the rigid blade. Simulating the blade using the rigid body feature in ABAQUS is important to monitor the reaction forces acting on blade. Figure 3.4 shows a sample of the meshing of the soil block. The blade angle is 90° and operating depth is 100 mm.

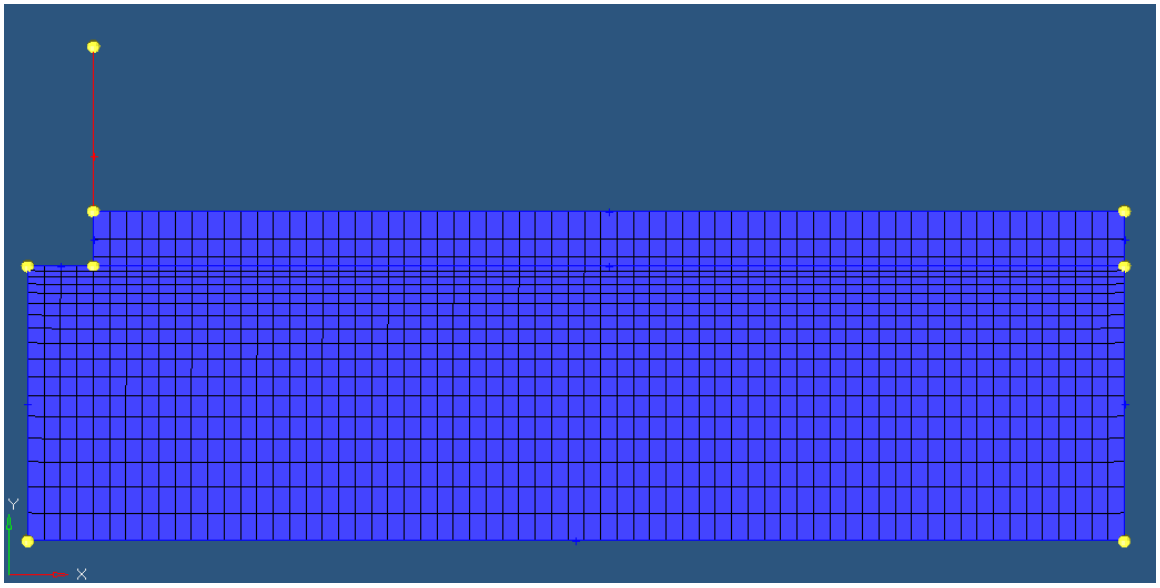

Figure 3.4 Finite element mesh of vertical cutting blade

The Coulomb friction model was used to describe friction at the soil-blade interface. The model relates the maximum allowable frictional (shear) stress across an interface to the contact pressure between the contacting bodies. In the basic form of the Coulomb friction model, two contacting surfaces can carry shear stresses up to a certain magnitude across their interface before they start sliding relative to one another; this state is known as sticking. The Coulomb friction model as shown in Equation (3.30) defines this critical shear stress, τ_{crit}, at which sliding of the surfaces starts as a fraction of the contact pressure, P_n, between the contacting surfaces.

$$\tau_{crit} = \beta P_n \tag{3.40}$$

The soil-blade interaction was simulated by element-based surface-to-surface (master-slave relationship) contact pair interaction as discussed in Sections 3.3.1.3 and 3.3.1.4. ABAQUS recommends the use of the stiffer body as the master surface for numerical efficiency. The rigid blade body chosen as a master surface was in contact with the deformable soil. The deformable soil was selected as a slave surface. As the master surface moved past the deformable slave surface, the shear and normal forces across this interface were computed. The relative motion of the two surfaces was modeled using a small sliding formulation which assumes that although two bodies may undergo large motions, there will be relatively little sliding of one surface along the other (ABAQUS, 2010). The following boundary conditions were used in the analyses:

1. Bottom base nodes are constrained in the vertical direction.
2. The two nodes at the bottom corners of the block were constrained on all degree of freedom
3. Nodes along both sides are constrained in the horizontal direction.
4. All other nodes are free in both translation and rotation
5. The blade is constrained in vertical direction and rotation but it is free to displace in the horizontal direction.

A geostatic step was first performed to assign initial stress level within the soil profile. The weight of the blade was not considered in the analysis. ABAQUS uses an incremental method to solve the material non-linearity. The total horizontal movement of the blade is divided into small increments. During each increment, a single-step Newton-Raphson iteration method is used to solve equilibrium equations.

3.4.4. Model Validation. The validation of the soil-blade interface model was achieved through an investigation of:

- Soil failure surface
- Soil displacement fields

A vertical blade operating at a depth of 100 mm was used for the validation of the model. The total number of soil elements was 1,475 with 1,557 nodes, resulting in 3,121 equations and 3,127 variables (degrees of freedom plus maximum number of any Lagrange multiplier variable). A total blade displacement of 30 mm was applied

incrementally throughout the simulation. The total number of iterations was 38 at a run time of 31.3 seconds. The failure surface and displacement fields obtained from the model were compared with previous experimental as well as finite element models of the soil cutting process.

3.4.4.1 Soil failure surface. The results show that the initial soil failure started around the bottom of the tool. As the load increased, the failure region extended around the blade tip then expanded towards the soil surface. The evolution of the failure surface is shown in the plastic strain plots (Figures 3.5). The failure zone formed a curved failure surface ahead of the soil. Chi and Kushwaha (1990) obtained a curved failure surface in front of the tool in the 3D FE analysis of the soil-blade interaction. The observation was especially true for the case of a blade with 90° rake angle. As can be seen from the plastic strain plots, the soil between the failure surface and the blade surface was in stable condition. This observation is in contrast to the assumption made in analytical methods (Terzaghi's passive earth pressure theory), where the soil within the failure region is considered to be in a state of plastic equilibrium. The result from the finite element analysis is in close agreement to real situation during soil cutting. It has been observed, both in field and laboratory experiment, that lumps of soil were left on the soil surface after soil cutting/excavation (Chi and Kushwaha, 1990; Payne, 1956). This is an indication that not all the soil ahead of the blade failed.

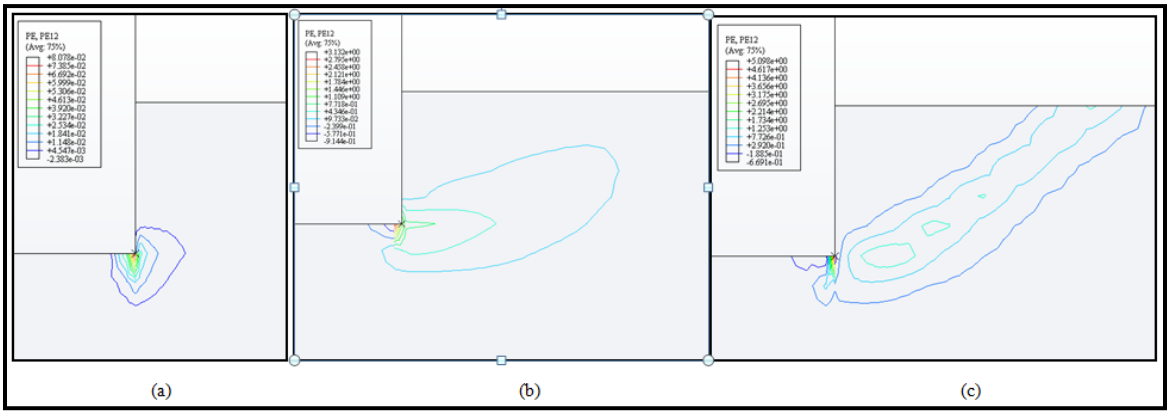

Figure 3.5 Plastic strains in soil at blade displacement of: (a) 0.75 mm; (b) 17.03 mm; and (c) 30 mm

3.4.4.2 Soil displacement fields. Figure 3.6 shows the displacement vectors of the soil elements at 30 mm of blade displacement. The size of the arrows is proportional to the magnitude of the displacement, and the arrow direction indicates the direction of soil displacement. The displacement direction of soil within the failure zone was upward to the right in the direction of blade movement. Outside the failure zone, the soil showed little movement and the direction was predominantly upwards. Experimental observations by Yong and Hanna (1977) verified the two zones depicted in the finite element analysis. FE modeling of soil tool interaction by Davoudi et al. (2008), Yong and Hanna (1977), and Chi and Kushwaha (1990) also predicted the same behavior. The maximum amount of displacement was found in the soil adjacent to the blade surface. The soil mass can be divided into two distinct regions from a displacement perspective: the region adjacent to the blade with significant amount of displacement, and region with little or no displacement. The line of separation between these two regions is the failure surface.

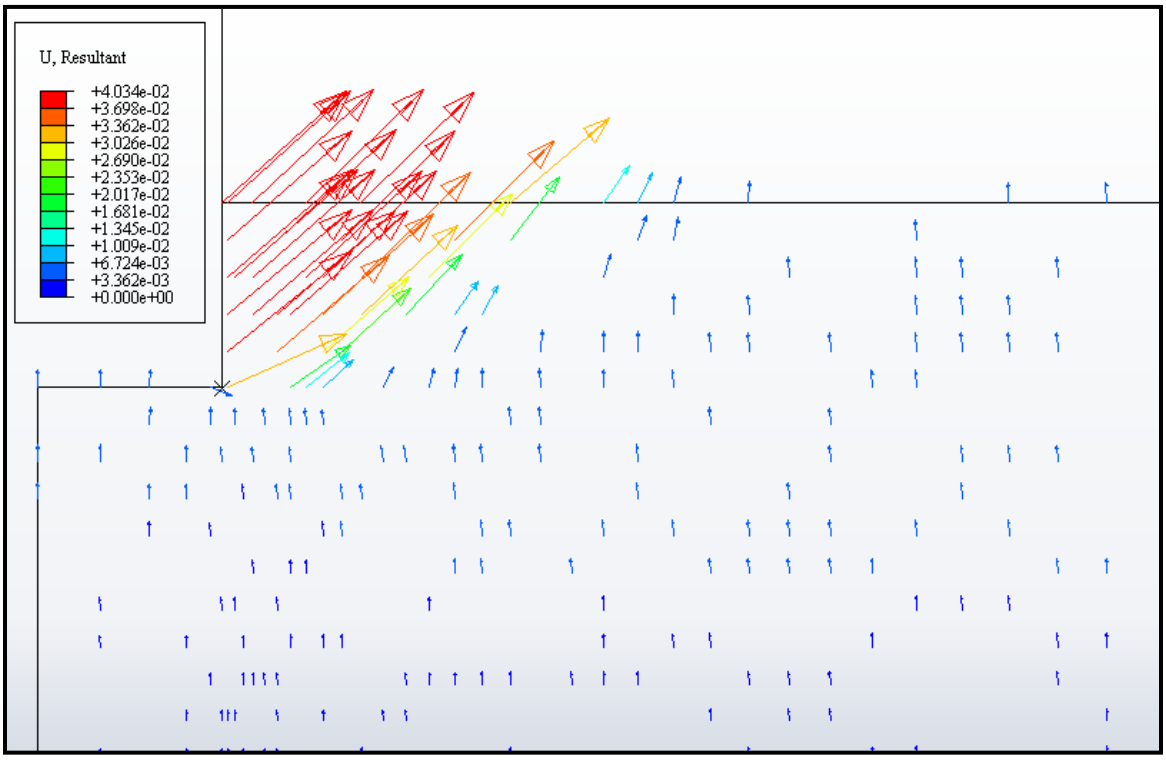

Figure 3.6 Soil displacement vectors at blade displacement of 30 mm

3.4.5. Sensitivity Analysis. A series of experiments were performed using the validated finite element model to study the effect of blade operating conditions and soil-blade interface friction on the cutting and vertical forces. The purpose of this study was to gain understanding into how these factors affect the cutting blade performance.

3.4.5.1 Effect of operating conditions. The soil-cutting blade model was used to study the effect of two operating conditions, which include the cutting depth and cutting angle on the cutting/vertical force. Table 3.2 presents the operating conditions used in simulating soil-tool interaction for the soil-blade model. The clayey soil properties contained in Table 3.1 were used throughout the analyses at a soil metal friction coefficient of 0.364. A total blade displacement of 20 mm was used for all scenarios. The two operating conditions were studied through a series of analyses, where the cutting depth and cutting angle (one at a time) were varied between the limits in Table 3.2.

Table 3.2 Operating conditions parameters

Cutting angle (degrees)	60			75			90		
Cutting depth (mm)	100	200	300	100	200	300	100	200	300

3.4.5.2 Effect of soil-blade friction. A certain amount of relative displacement always exists at the soil-tool interface during a continuous soil cutting process. The magnitude of this displacement depends on the roughness of the tool surface and the external friction and adhesion characteristics of the soil. A series of finite element experiments of soil-tool interaction was carried out to study the effect of soil-metal coefficient of friction on blade cutting/vertical force. Blade surface roughness is a design factor, which can be adjusted during blade manufacturing. Soil-metal friction coefficient is dependent on soil type as well. The various soil-tool friction coefficients considered in the analyses are 0.05, 0.1, 0.2 and 0.3. These analyses were carried out at a cutting angle of 90° and cutting depth of 100 mm. For each finite element simulation, the cutting and vertical forces were plotted through a blade displacement of 30 mm.

4. RESULTS AND DISCUSSIONS

This section contains detailed discussions of results obtained from the simulation experiment. The MCC soil properties and operating conditions of the blade are shown in Tables 3.1 and 3.2. All analyses are carried out on a Windows 7 machine with a 3 GHz Intel core 2 duo CPU and 4 GB of RAM memory. The average CPU time, including the pre-processing and solving, was 32 seconds.

4.1. SOIL BLADE INTERACTION

The results from the validated finite element model were used to gain understanding into the interaction between a cutting blade and soil. The analysis was carried out at blade angle of 90° and operating depth of 100 mm. The results of the model provided information on blade forces, soil deformation, soil displacement fields and blade stresses. A cutting blade had a total displacement of 30 mm.

4.1.1. Blade Forces. The reaction forces were calculated from the finite element analysis from a small displacement assigned to the reference node of the rigid blade at each increment. Force-displacement curves obtained from the finite element analysis are shown in Figure 4.1. The plain strain assumption calculates the cutting forces for a unit width of the blade. After about 16.5 mm of blade displacement, the draft force reached a maximum of 24.87 kN. That is an indication of a failure point within the soil. Further blade displacement beyond the peak cutting force resulted in a reduction of the cutting force. The reason for this reduction can be related to the soil failure formation, leading to lesser force required to continue the movement. The maximum/peak force was used as the force required for soil cutting.

The vertical forces were negative and that is an indication of a force tending to lift the cutting blade upward out of the soil. The maximum vertical force was about 2.58 kN. The cause of the initial tendency of the soil to push the blade upward can be related to the frictional forces acting on the blade after soil particles were moving upward. The soil elements displacement vectors at blade displacement of 17.6 mm is shown in Figure 4.2.

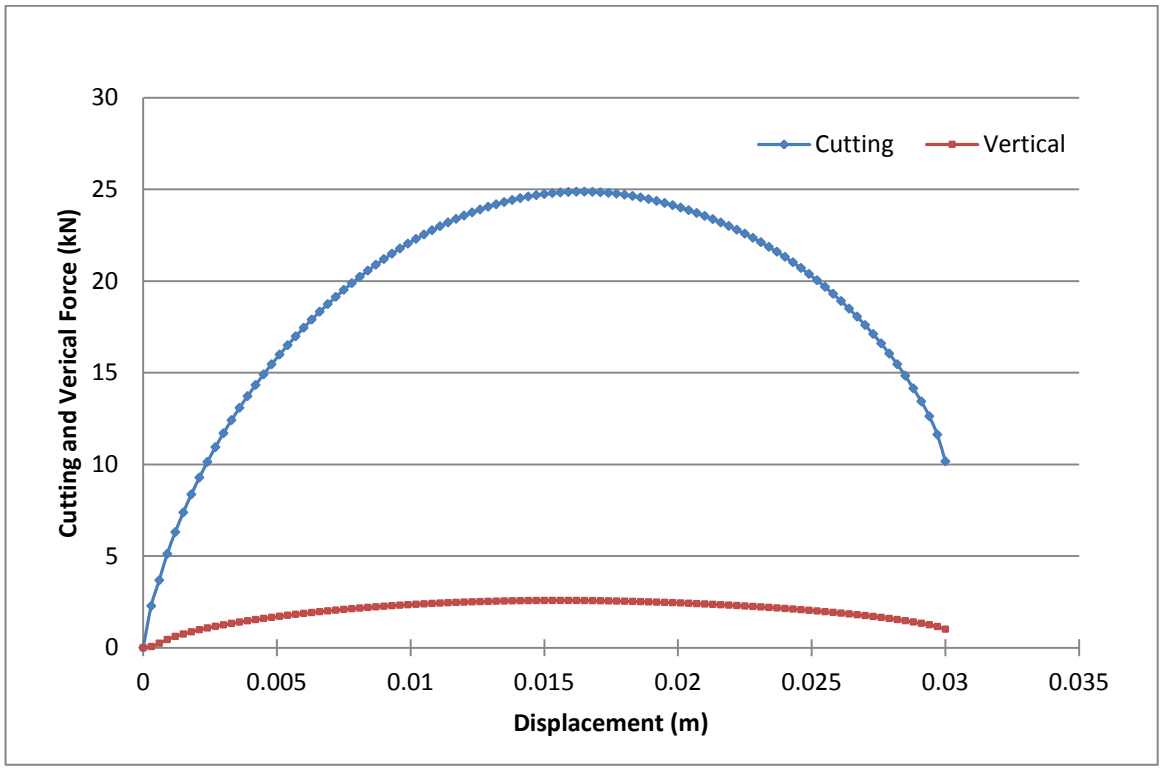

Figure 4.1 Reaction forces acting on the cutting blade versus displacement

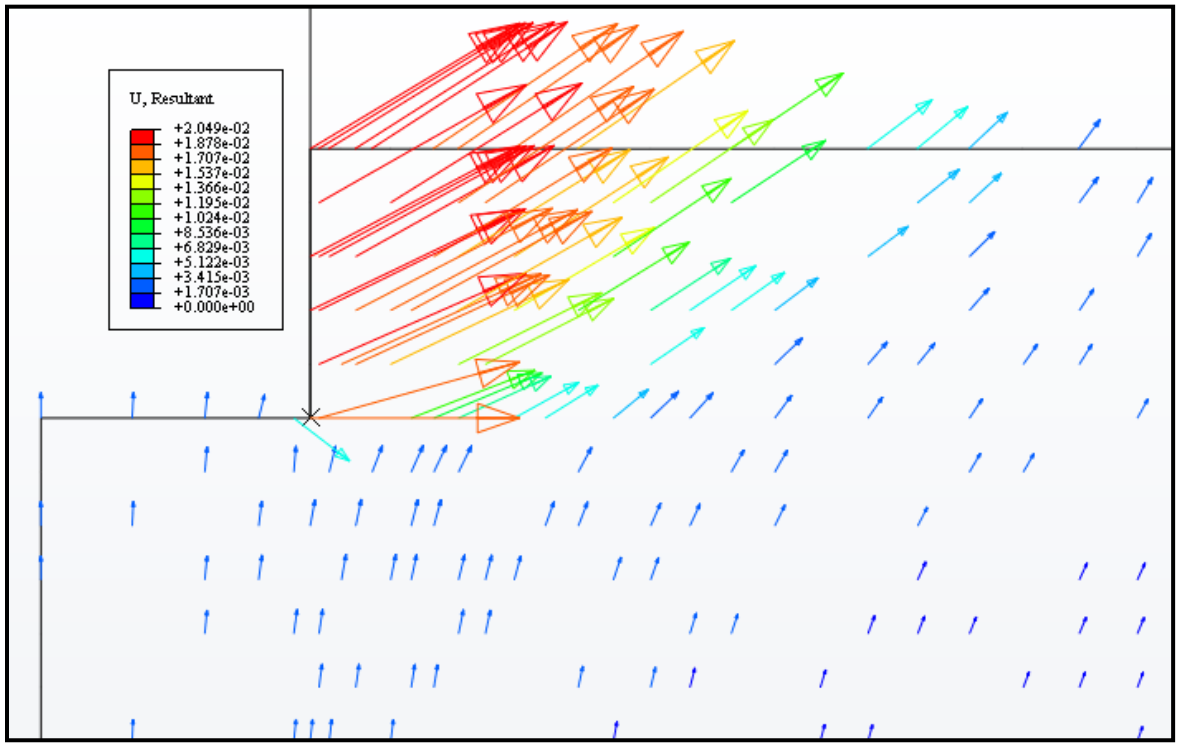

Figure 4.2 Soil displacement vectors at blade displacement of 17.6 mm

The figure shows that the soil displacements beneath the blade tip and adjacent to the blade have upward components. The reduction in the vertical force can be caused by loosening of the soil in the vicinity of the blade after the soil failure point was reached.

4.1.2. Blade Stresses. The stress distribution (contact pressure) on the surface of the cutting blade at 30 mm of blade displacement is shown in Figure 4.3.

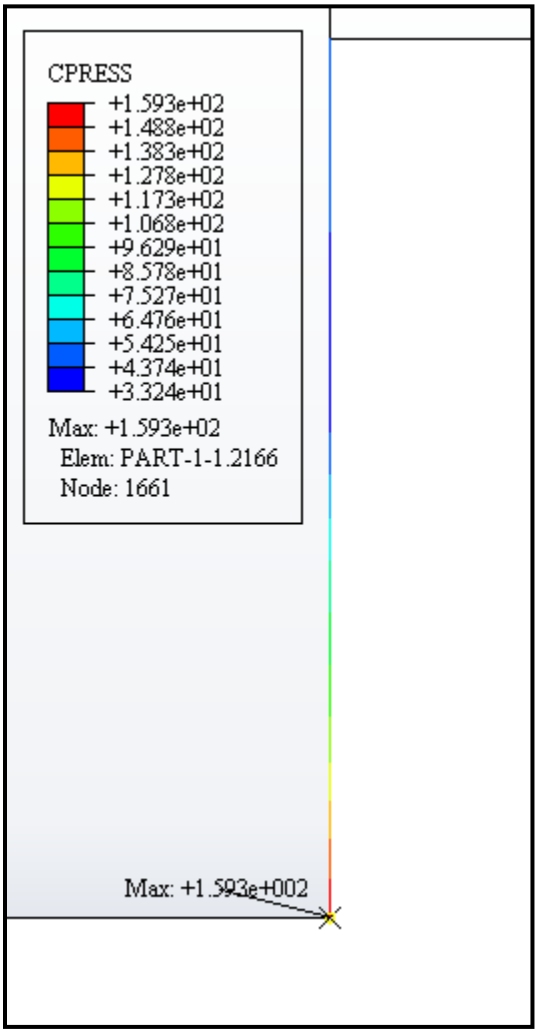

Figure 4.3 Contact pressure distribution on cutting blade at displacement of 30 mm

The maximum blade stress was found at the tip of the cutting blade at 159.3 kPa. This is because the normal stress is highest at the blade tip. Maximum wear of the blade is expected to occur at this point since it has the highest stress.

4.2. SENSITIVITY ANALYSIS

This section presents the effects of changes in blade cutting depth and angle on the magnitude of the cutting or vertical force of blade. Also presented and discussed, is the effect of changes in soil-blade coefficient of friction on blade cutting or vertical force.

4.2.1. Effect of Cutting Depth. Firstly. the effect of cutting depth was investigated at various blade cutting angles. Thus, for each blade cutting angle of 60°, 75° and 90°, three separate finite element models were run with cutting depths of 100, 200 and 300 mm. Cutting force-displacement curves obtained from the finite element analysis are shown in Figures 4.4, 4.5 and 4 6. The figures represent the effect of cutting depth on blade cutting forces in the horizontal direction. From Figure 4.4, at a blade angle of 60°, the maximum cutting force increased by 142.6% from a cutting depth of 100 mm to 300 mm. It, however, increased by 139.6% and 124.4% for blade angles of 75° (Figure 4.5) and 90° (Figure 4.6), respectively. The percentage increase in the blade cutting force due to cutting depth reduced as the operating angle of the blade increased from 60° to 90°.

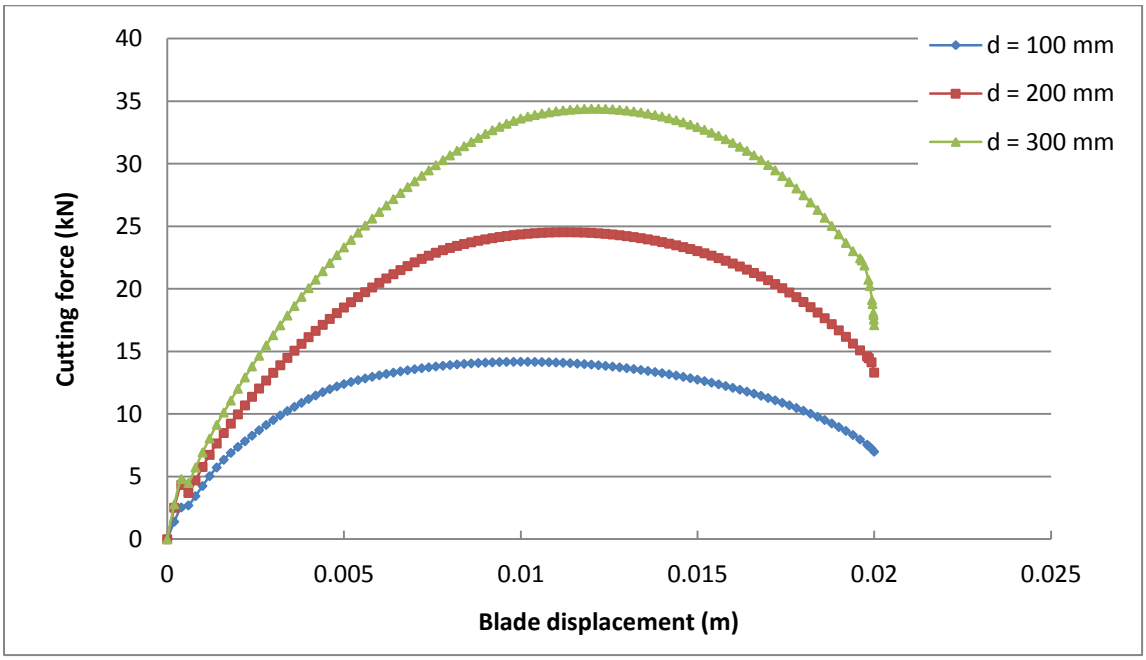

Figure 4.4 Effect of cutting depth on cutting force at cutting angle of 60°

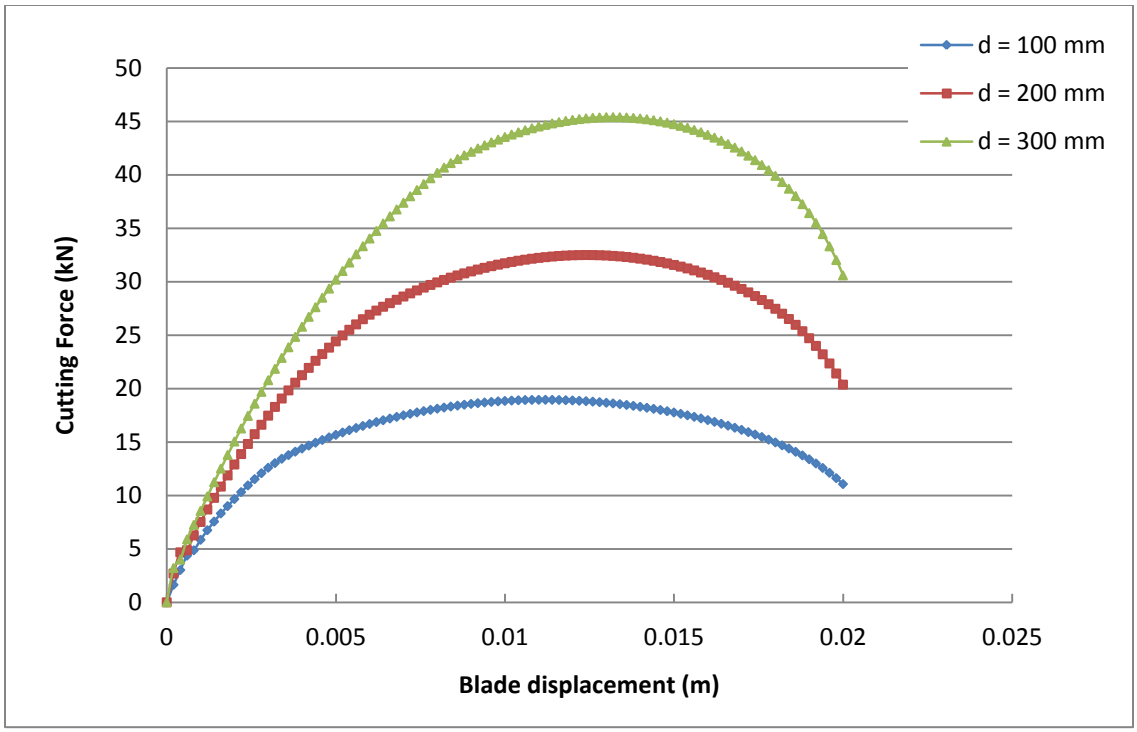

Figure 4.5 Effect of cutting depth on cutting force at cutting angle of 75°

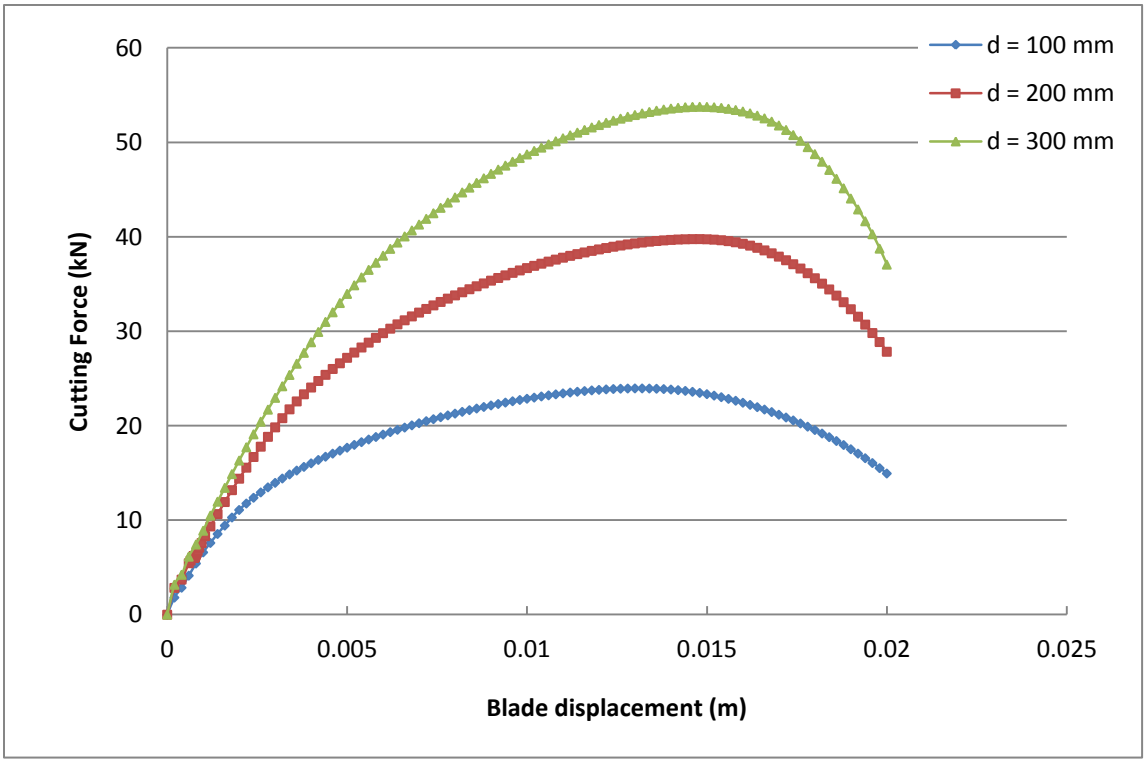

Figure 4.6 Effect of cutting depth on cutting force at cutting angle of 90°

A summary of the relationship between the peak cutting force and cutting depth is presented in Figure 4.7. It is clear that, for each cutting angle, the blade cutting force increases with increasing cutting depth. This observation is due to the increase in normal pressures at the soil failure plane as cutting depth increases. The shearing resistance of soil at the cutting plane increases with increasing normal pressures. Increasing the operating depth of the blade also increases the area of contact between the blade and soil. This increases the frictional resistance at the soil-blade contact.

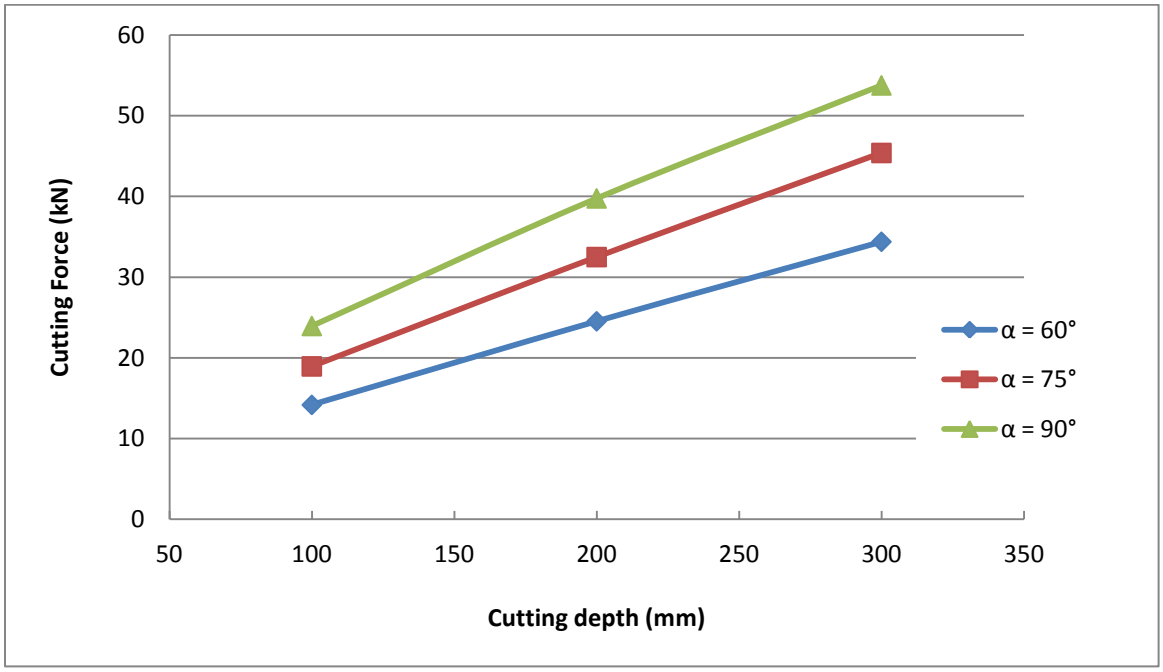

Figure 4.7 Maximum cutting force versus cutting depth at various cutting angles

The effect of cutting depth on the blade vertical force is shown in Figures 4.8, 4.9 and 4.10. At a blade angle of 60°, the vertical force increased from 2.4 kN to 6.03 kN at a depth of 100 mm to 300 mm. The direction of the vertical force changed at angles of 75° and 90° as shown in Figures 4.9 and 4.10. However, their magnitudes increased with depth (from 100 mm to 300 mm). The soil exerts a lifting/upward force on the blade when the blade angle is 75° and 90° to the horizontal. The vertical force increased by 126.6% and 113.6% for 75° and 90°, respectively. It can be concluded from the results that the blade vertical force increases with cutting depth.

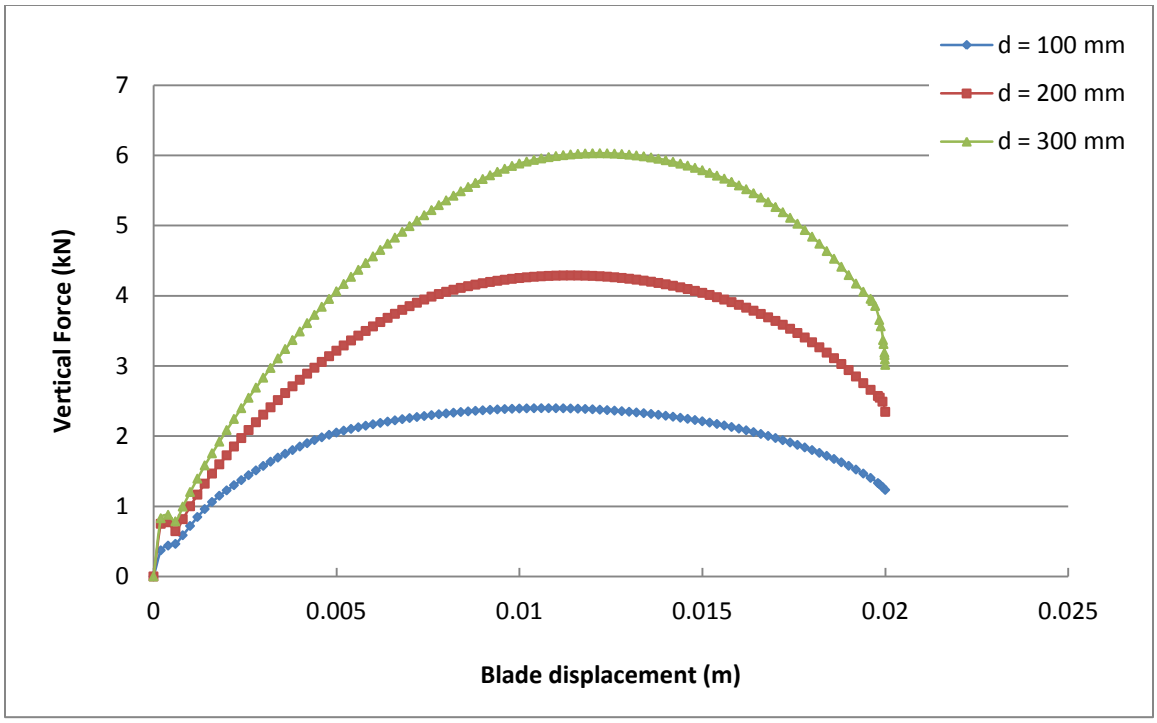

Figure 4.8 Effect of cutting depth on vertical force at cutting angle of 60°

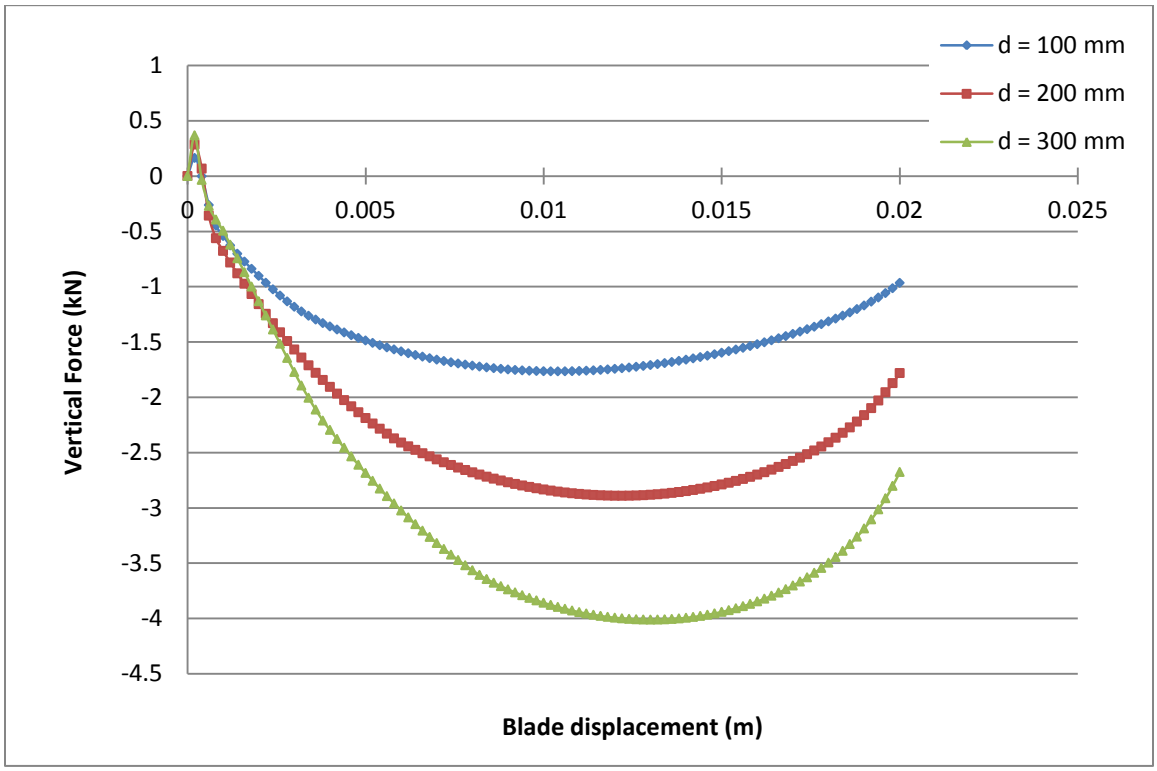

Figure 4.9 Effect of cutting depth on vertical force at cutting angle of 75°

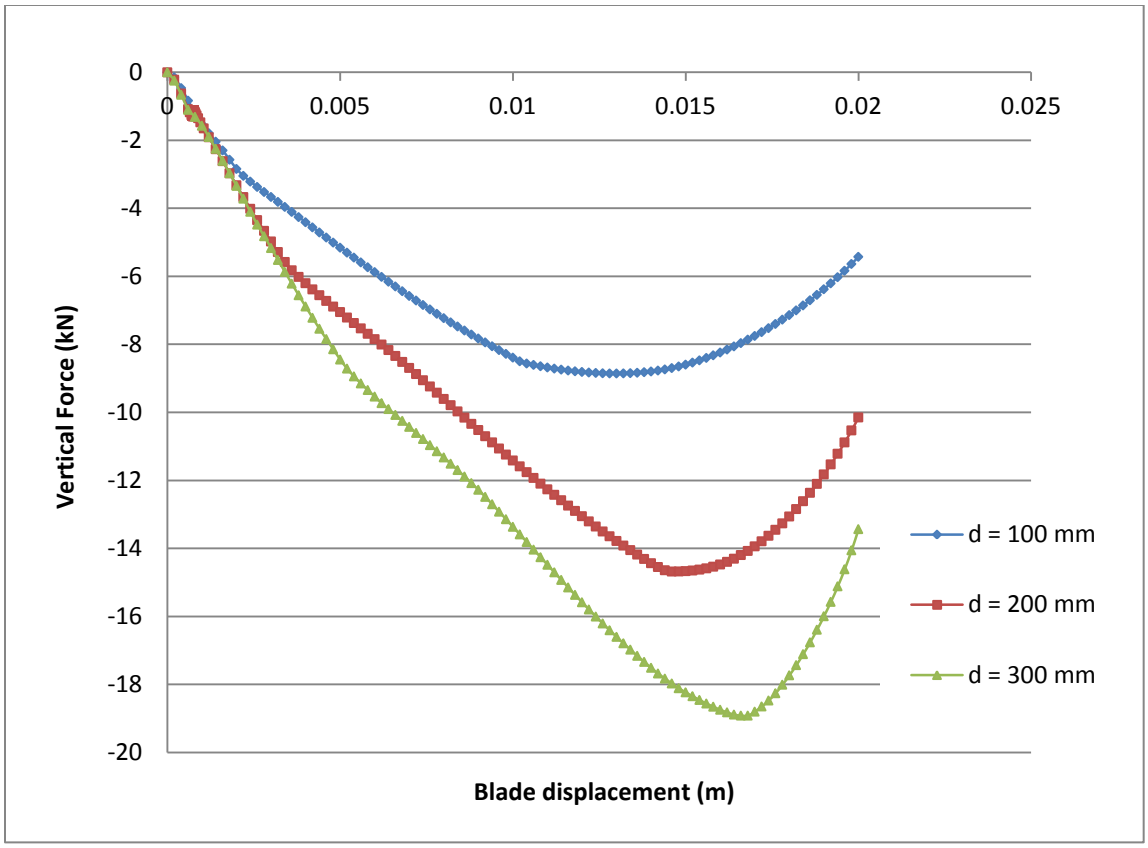

Figure 4.10 Effect of cutting depth on vertical force at cutting angle of 75°

4.2.2. Effect of Cutting Angle. The effect of cutting angle was investigated at various blade cutting depths. Thus, for each blade cutting angle, three separate finite element models were run with cutting depths of 100, 200 and 300 mm. The effects of cutting angles at 60°, 75° and 90° on blade cutting force are shown in Figures 4.11, 4.12 and 4.13, respectively. Figure 4.11 shows that the cutting force increases with increasing blade angle at 100 mm of cutting depth. The cutting force increased from 14.2 kN to 24 kN at a blade angle of 60° to 90°. Similar relations between cutting force and blade angle were obtained at 200 mm and 300 mm operating depths as shown in Figures 4.12 and 4.13, respectively. The cutting force increased by 62% and 56% for cutting depths of 200 mm and 300 mm, respectively. The percentage increase in the blade cutting force reduced as the operating depth of the blade increased.

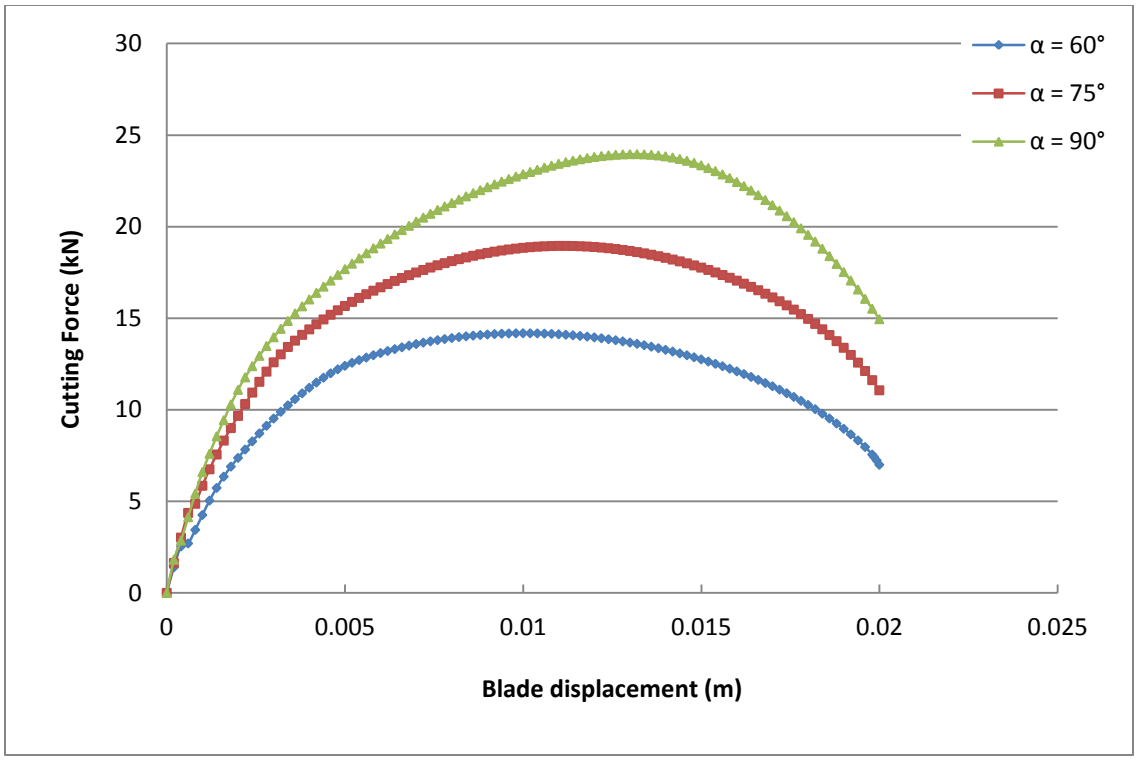

Figure 4.11 Effect of cutting angle on cutting force at blade displacement of 100 mm

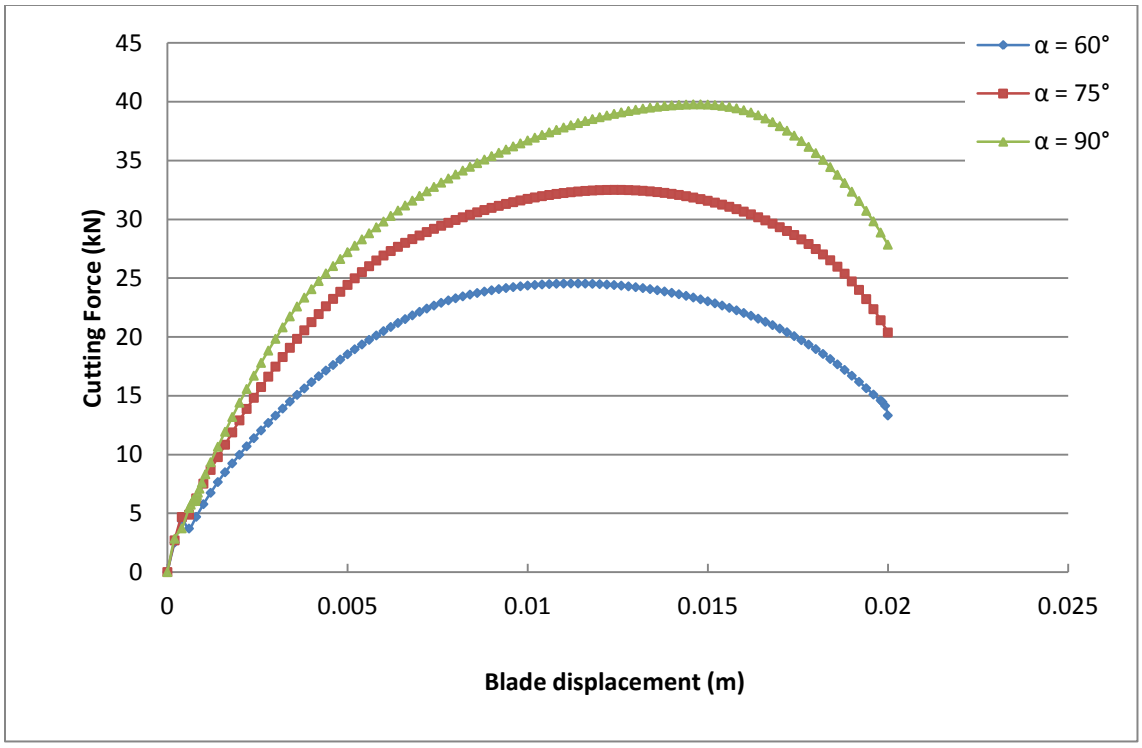

Figure 4.12 Effect of cutting angle on cutting force at blade displacement of 200 mm

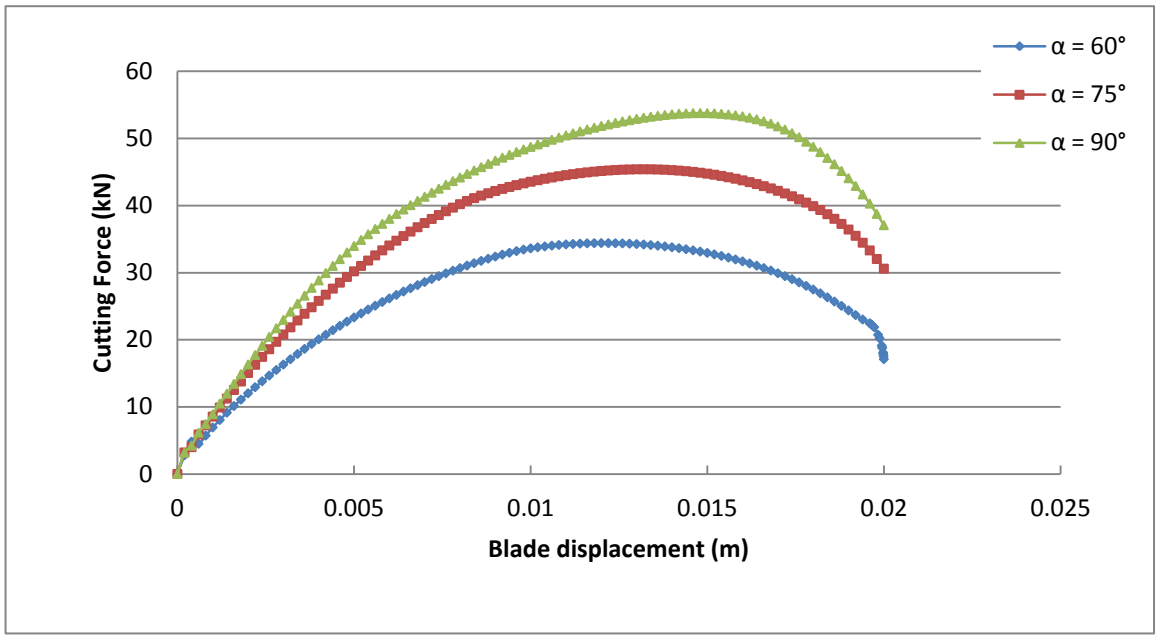

Figure 4.13 Effect of cutting angle on cutting force at blade displacement of 300 mm

The relationship between cutting force and cutting angle is summarized in Figure 4.14. It is clear that, for a given cutting depth, the blade cutting force increases with increasing

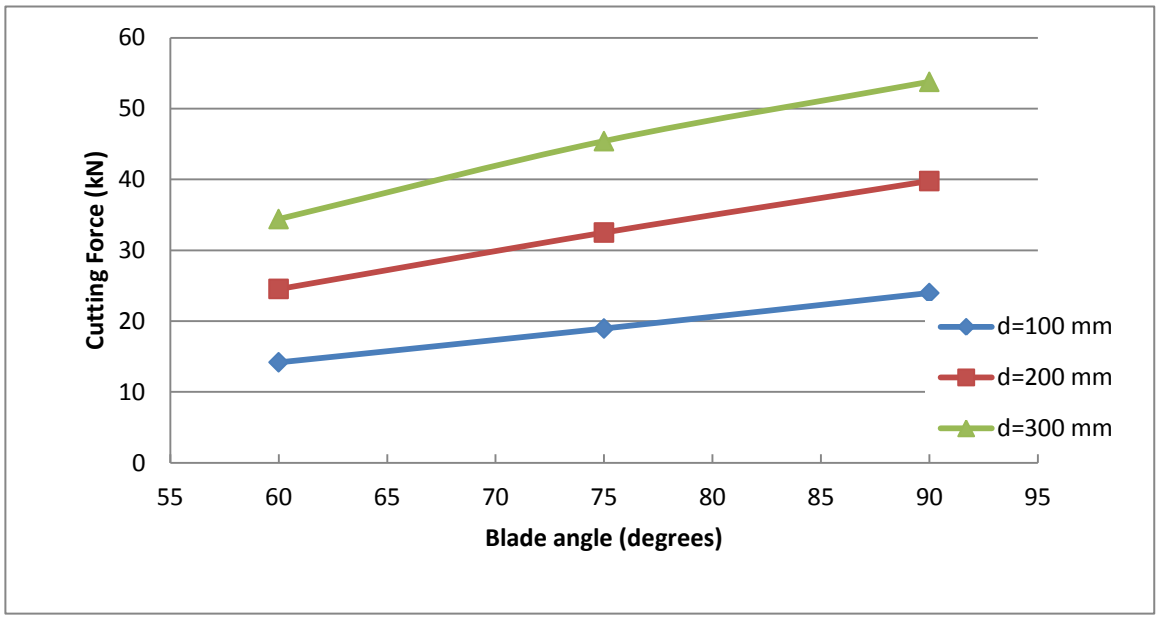

Figure 4.14 Peak cutting force versus cutting angle at various cutting depths

blade angle. Increasing the cutting angle of the blade increases the volume of the cut soil and as a result, the normal pressure on the failure surface. The shearing resistance of the soil increases as the normal pressure on the shearing plane increases.

The effects of cutting angles at 60°, 75° and 90° on blade vertical force are shown in Figures 4.15, 4.16 and 4.17, respectively. The figures show that both the direction and magnitude of the vertical force change as a function of the blade angle. The soil exerts a lifting/upward force on the blade when the blade angle is 75° and 90° to the horizontal. This is evident from the sign of the vertical force. In all the vertical force versus blade displacement plots, the magnitude of the force at a blade angle of 90° was greater than those at 75°. The vertical force is acting downward for cutting blade angle of 60°.

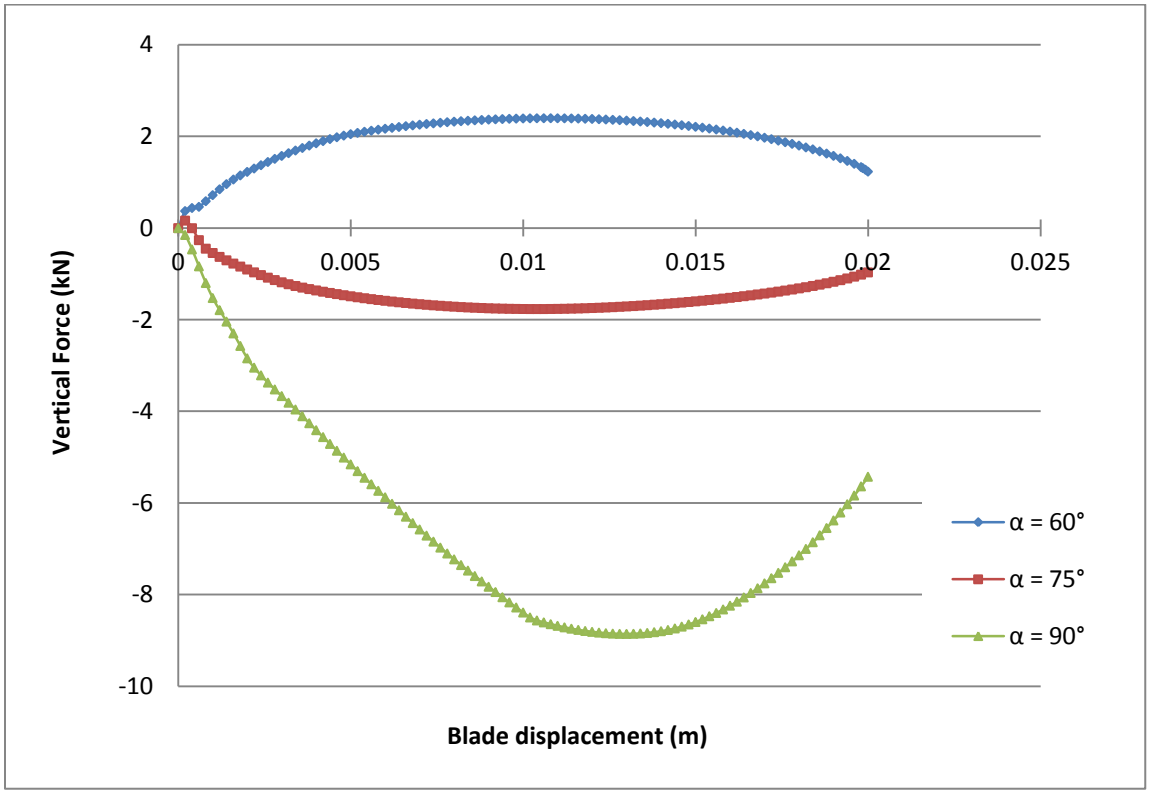

Figure 4.15 Effect of cutting angle on vertical force at blade displacement of 100 mm

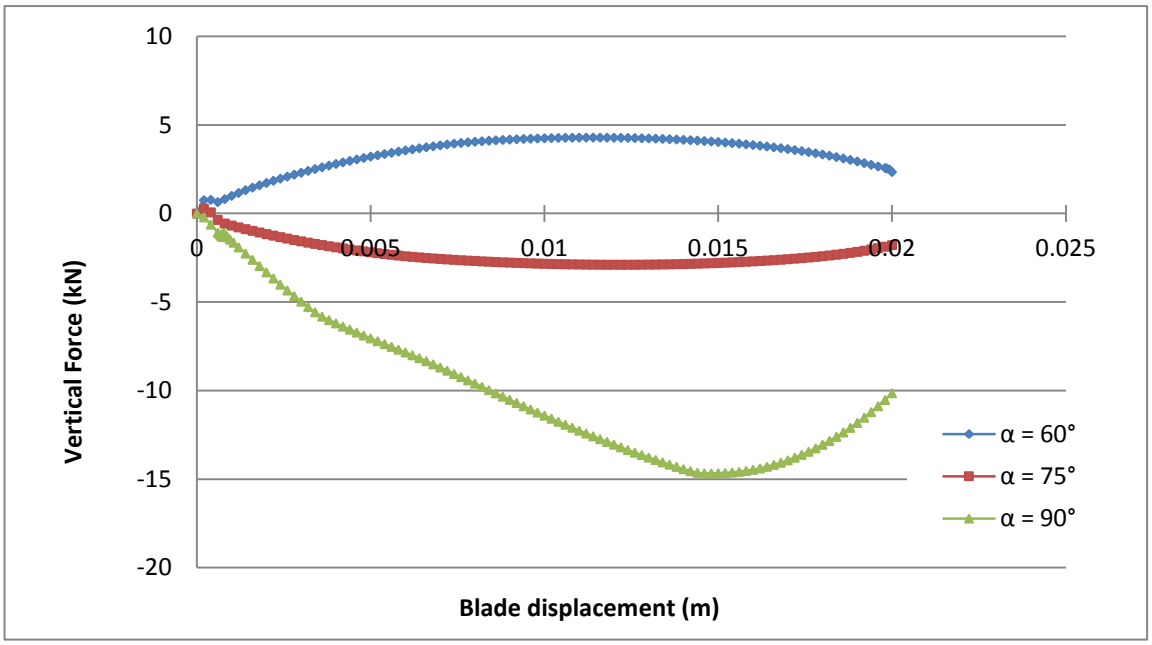

Figure 4.16 Effect of cutting angle on vertical force at blade displacement of 200 mm

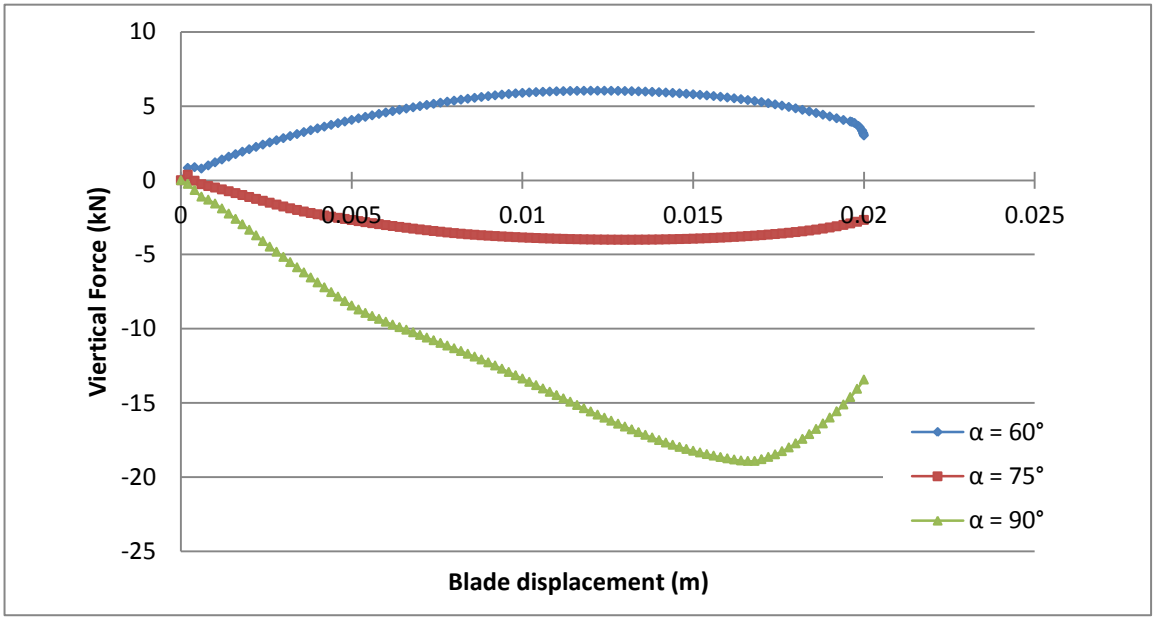

Figure 4.17 Effect of cutting angle on vertical force at blade displacement of 300 mm

Figure 4.18 shows a summary of the relationship between vertical force and blade angle at various operating depths. It is clear from the graph that, the transition from a lifting to a downward vertical force will occur at a blade angle of about 70°. The angle at which the transition occurs is dependent on the soil-blade friction and the cutting angle.

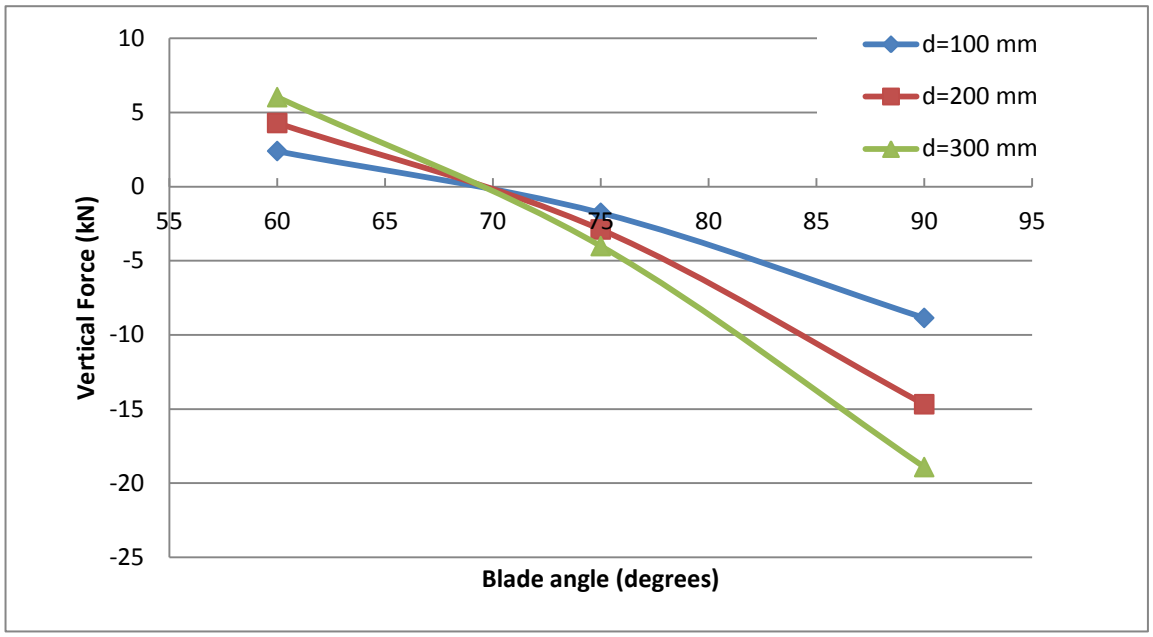

Figure 4.18 Relationship between vertical force and blade angle

4.2.3. Effect of Soil-Blade Friction. According to Shen and Kushwaha (1998), it is difficult to use experimental methods to comprehend the extent of maximum potential savings in cutting force for different tools and soil conditions by eliminating or reducing the friction at the interface. The finite element method is capable of predicting the potential gain/loss in cutting force due to changes in friction at the interface. The FE model developed was used to study the effect of soil-metal coefficient of friction on blade cutting/vertical force. For each finite element simulation, the cutting and vertical forces were plotted through a blade displacement of 30 mm. Figure 4.19 shows the effect of friction coefficient on blade cutting force. The cutting force increases with increasing coefficient of friction. There is minimal or no effect of the coefficient of friction on the cutting force at small blade displacement (up to about 5 mm). The effect of friction is apparent at higher displacement when there is significant accumulation of soil ahead of the blade surface. Reducing the coefficient of friction at the soil-blade interface from 0.3 to 0.05 reduces the maximum cutting force by 22.3%. The percentage represents the maximum potential savings in blade cutting force by reducing the coefficient of friction.

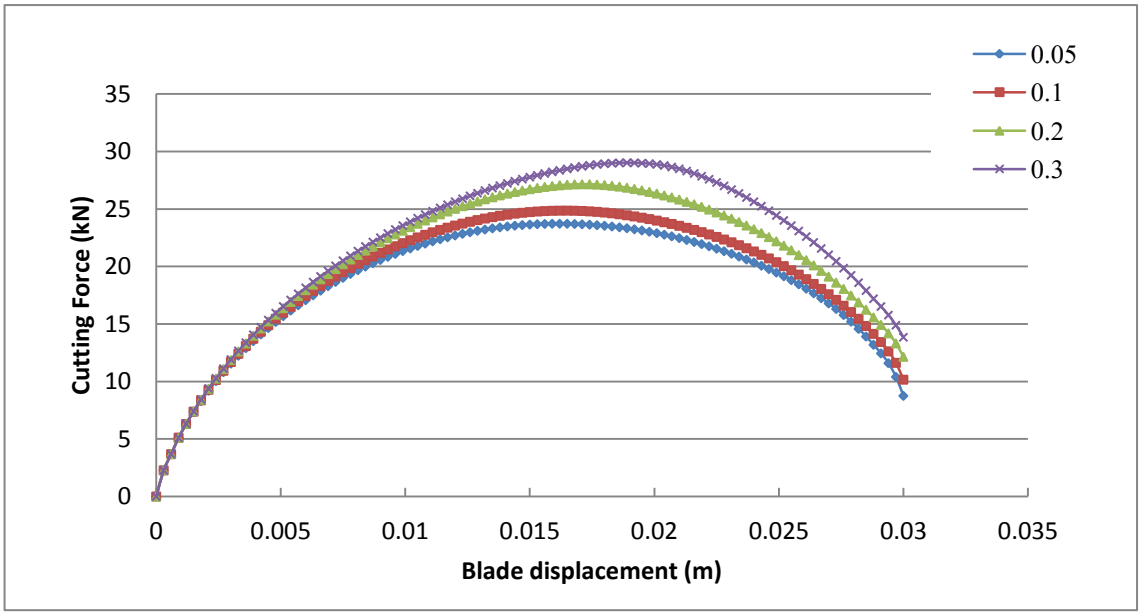

Figure 4.19 Effect of soil-metal coefficient of friction on cutting force

A similar relationship for blade vertical force is observed from Figure 4.20. The coefficient of friction at the soil-blade interface has a greater effect on blade vertical force than the cutting force. Increasing the friction coefficient from 0.05 to 0.3 increases the vertical force from 1.27 kN to 8.83 kN. This represents about 596% increase in the vertical force.

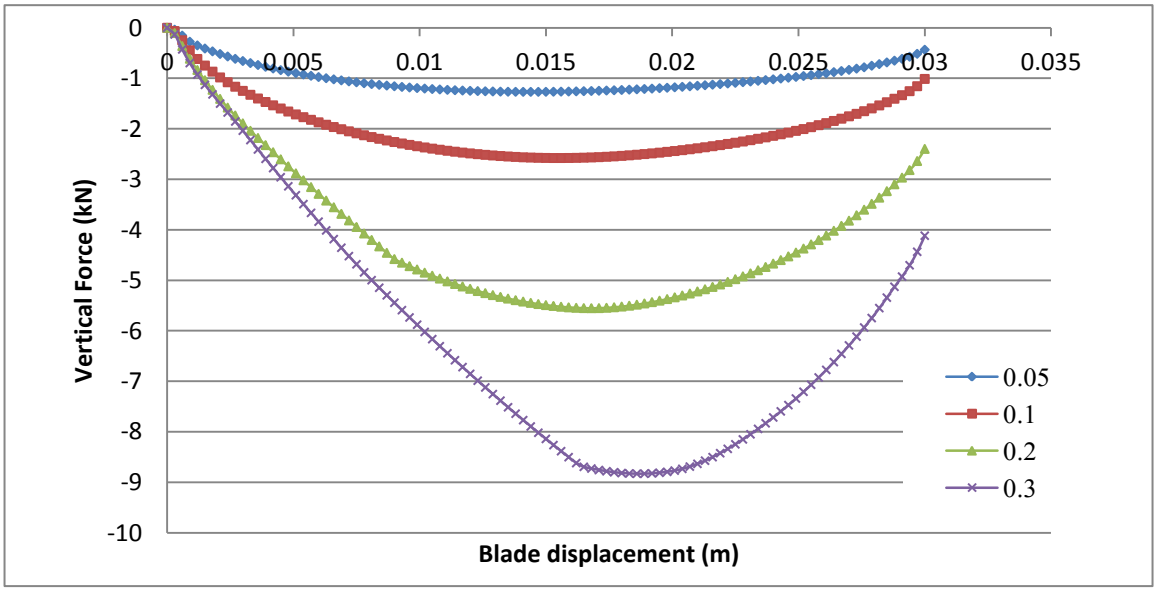

Figure 4.20 Effect of soil-metal coefficient of friction on vertical force

5. SUMMARY, CONCLUSIONS AND RECOMMENDATIONS

This chapter summarizes the work presented throughout this thesis and provides appropriate conclusions and recommendations for future research initiatives in this area.

5.1. SUMMARY

Excavation and loading are major primary operations in the surface mine production chain, constituting a significant component of the production cost (Tons et al., 2004). Thus, excavation and loading are important cost centers that need to be improved to lower production costs and improve overall energy efficiency. Optimization of tool design will help to improve energy efficiency in earthmoving operations. Accurate modeling of soil-implement interaction is the basic key to this optimization.

Empirical (Payne, 1956; Aboelnor et al., 1998; Mouazen and Nemenyi, 1999, Rosa and Wulfsohn, 1999) and analytical (Osman, 1964; Reece, 1965, Mckyes and Ali, 1977; Perumpral et al., 1983; Swick and Perumpral, 1988) methods have been used to conduct parametric studies of soil-tool interaction for modeling energy requirement of tillage and excavation operations. These methods have been successful to some extent, however, they can hardly be extended to a general case because of the underlying assumptions and simplification of tool shapes. Modeling soil-tool interaction using finite element analysis produces some advantages over other modeling methods. In this case, any tool structure and the non-linear behavior of the cutting tool interaction can be modeled if a proper constitutive law is chosen (Kushwaha and Zhang, 1998). The soil constitutive equations used in most of the available FEM analysis of soil-blade interaction fail to adequately model the elastic and plastic behavior of soil. As a result, soil-blade interaction modeling with a nonlinear elasto-plastic soil constitutive model is still an emerging research frontier.

Finite element modeling techniques were used to study the behavior of formation-blade interactions in excavation. The mechanical behavior of the soil was modeled as a non-linear elasto-plastic material using the Modified Cam Clay (MCC). The MCC is an elasto-plastic strain hardening model, capable of modeling the non-linear behavior of soil

by means of hardening plasticity. The MCC model is based on the critical state soil mechanics. Coulomb friction model was used to describe friction at the soil-blade interface.

The geometry and meshing of the finite element model was generated using HyperMesh (Altair HyperWorks, 2009). Simulation and post-processing of the model was performed with the finite element commercial package ABAQUS (2010). An incremental method based on the single-step Newton iteration algorithm was used to solve the finite element equilibrium equations. The developed FE model was validated by qualitatively comparing the results from the analysis and from previous experimental and numerical methods.

Detailed analysis of the simulation results is carried out to investigate the interaction between the cutting blade and soil. The results provided soil forces, a progressive developed failure zone, displacement fields and stress distribution along the tool surface. The effects of the cutting blade operating conditions and soil-blade interface property on machine performance were studied.

5.2. CONCLUSIONS

This study combined the use of an analytical literature review, finite element mathematical and computer modeling, and detailed analysis of numerical results to achieve the objectives of this research endeavor. The formation was modeled as a non-linear elasto-plastic material using the Modified Cam-Clay model. The model was validated with previous experimental and finite element models of soil-tool interaction.

From detailed experimentation and analysis of results from the finite element model of the soil-blade interaction, the following conclusions have been drawn:

1) The soil failure surface was found to initiate from the blade tip, and extended to the soil surface as loading increased.

2) Two distinct soil regions were observed from the displacement vectors: the region adjacent to the blade with significant amount of displacement, and region with

little or no displacement. The maximum amount of displacement was found in the soil sliding on the blade surface.

3) The cutting force of the blade increased to a maximum as the blade was pushed against the formation. This was an indication of a failure point within the soil. Further blade displacement beyond the peak force resulted in a reduction of the cutting force.

4) The maximum blade stress was found at the tip of the cutting blade. Maximum wear of the blade is expected to occur at this point since it has the highest stress.

5) For each cutting angle, the blade cutting force increases with increasing cutting depth. At a blade angle of 60°, the maximum cutting force increased by 142.6% from a cutting depth of 100 mm to 300 mm. It however increased by 139.6% and 124.4% for blade angles of 75° and 90°, respectively.

6) The sensitivity analysis of changes in blade angle on cutting force showed that, the cutting force increases with increasing blade angle. At cutting depth of 100 mm, the cutting force increased from 14.2 kN to 24 kN at a blade angle of 60° to 90°. The cutting force increased by 62% and 56% for cutting depths of 200 mm and 300 mm, respectively.

7) The direction and magnitude of the vertical force change as a function of the blade angle and the soil-blade friction coefficient. The soil exerts a lifting force on the blade at a friction coefficient of 0.364 and cutting angles greater than 70°.

8) Increasing the coefficient of friction at the soil blade interface increases the blade cutting force. The analysis showed that reducing the coefficient of friction at the soil blade interface from 0.3 to 0.05 reduces the cutting force by 22.3%. The percentage represents the maximum potential savings in blade cutting force. The coefficient of friction at the soil-blade interface has a greater effect on blade

vertical force than the cutting force. The vertical force increased by 596% for coefficient of friction of 0.3 to 0.05.

5.3. RECOMMENDATIONS FOR FUTURE RESEARCH

Although this research study has made a significant progress in soil-blade interaction by accounting for both elastic and plastic behaviors of soils, several areas require improvements through further research. The following areas are recommended for future studies:

1) To validate the finite element model's ability to predict the blade cutting force, field or laboratory experimentation should be conducted to acquire necessary data for comparison.

2) The weight of the blade should be accounted for in the finite element model.

3) The dynamic effects of the soil-blade interaction process should be accounted for in the model. This will provide information on the effects of blade cutting speed and acceleration on machine performance.

4) Three-dimensional FE model of the interaction between a narrow cutting blade and soil could significantly improve and add to the body of knowledge in this research area. A 3D model would account for blade side effects.

5) Although FEM of soil-blade interaction provides some advantage over experimental and analytical methods, the FEM is mostly suitable for continuous analysis. The discrete element method which models the behavior of granular materials is more suitable for modeling soils and interactions between soil and rigid or flexible bodies. The capability of focusing on the microstructure level enriches the understanding of soil-tool interaction processes and enables the improvement of machinery design.

APPENDIX

SENSITIVITY ANALYSIS RESULTS

Effect of Cutting Depth on Blade Cutting Force (kN) at Cutting Angle of 90°

	Cutting depth		
Displacement (mm)	**100 mm**	**200 mm**	**300 mm**
0.00	0.00	0.00	0.00
0.40	2.85	3.72	4.22
0.80	5.42	6.37	7.43
1.20	7.59	9.34	10.49
1.60	9.43	11.93	13.42
2.00	11.09	14.40	16.32
2.40	12.38	16.70	19.10
2.80	13.48	18.83	21.71
3.20	14.42	20.81	24.18
3.60	15.26	22.58	26.57
4.00	16.02	24.05	28.84
4.40	16.73	25.40	31.00
4.80	17.37	26.62	33.00
5.20	17.98	27.75	34.87
5.60	18.55	28.81	36.51
6.00	19.08	29.81	38.01
6.40	19.57	30.74	39.40
6.80	20.05	31.58	40.68
7.20	20.49	32.37	41.91
7.60	20.91	33.11	43.08
8.00	21.29	33.81	44.17
8.40	21.66	34.46	45.22
8.80	21.99	35.08	46.20
9.20	22.31	35.65	47.12
9.60	22.60	36.19	47.96
10.00	22.86	36.70	48.73

	Cutting depth		
Displacement (mm)	**100 mm**	**200 mm**	**300 mm**
10.40	23.11	37.17	49.45
10.80	23.33	37.60	50.12
11.20	23.52	37.99	50.75
11.60	23.68	38.35	51.32
12.00	23.81	38.68	51.84
12.40	23.89	38.96	52.31
12.80	23.95	39.20	52.72
13.20	23.96	39.41	53.07
13.60	23.92	39.57	53.36
14.00	23.84	39.68	53.58
14.40	23.70	39.75	53.72
14.80	23.48	39.77	53.77
15.20	23.20	39.71	53.72
15.60	22.85	39.55	53.56
16.00	22.44	39.27	53.28
16.40	21.97	38.84	52.84
16.80	21.45	38.26	52.20
17.20	20.88	37.53	51.32
17.60	20.25	36.65	50.17
18.00	19.55	35.62	48.76
18.40	18.80	34.44	47.09
18.80	17.96	33.09	45.14
19.20	17.06	31.55	42.90
19.60	16.06	29.82	40.28
20.00	14.95	27.84	37.06

Effect of Cutting Angle on Blade Cutting Force (kN) at Cutting Depth of 100 mm

	Cutting angle		
Displacement (mm)	**60°**	**75°**	**90°**
0.00	0.00	0.00	0.00
0.40	2.54	3.02	2.85
0.80	3.44	4.87	5.42
1.20	5.04	6.75	7.59
1.60	6.35	8.32	9.43
2.00	7.37	9.67	11.09
2.40	8.28	10.94	12.38
2.80	9.13	12.08	13.48
3.20	9.89	13.03	14.42
3.60	10.58	13.78	15.26
4.00	11.20	14.39	16.02
4.40	11.75	14.93	16.73
4.80	12.21	15.43	17.37
5.20	12.57	15.89	17.98
5.60	12.85	16.31	18.55
6.00	13.10	16.69	19.08
6.40	13.31	17.04	19.57
6.80	13.50	17.35	20.05
7.20	13.67	17.64	20.49
7.60	13.80	17.89	20.91
8.00	13.92	18.12	21.29
8.40	14.01	18.32	21.66
8.80	14.08	18.49	21.99
9.20	14.13	18.64	22.31
9.60	14.17	18.75	22.60
10.00	14.18	18.84	22.86

	Cutting angle		
Displacement (mm)	**60°**	**75°**	**90°**
10.40	14.17	18.91	23.11
10.80	14.14	18.94	23.33
11.20	14.10	18.95	23.52
11.60	14.03	18.93	23.68
12.00	13.95	18.89	23.81
12.40	13.85	18.82	23.89
12.80	13.74	18.73	23.95
13.20	13.60	18.61	23.96
13.60	13.45	18.47	23.92
14.00	13.27	18.30	23.84
14.40	13.08	18.10	23.70
14.80	12.87	17.88	23.48
15.20	12.63	17.64	23.20
15.60	12.38	17.36	22.85
16.00	12.10	17.05	22.44
16.40	11.79	16.71	21.97
16.80	11.46	16.34	21.45
17.20	11.10	15.93	20.88
17.60	10.70	15.47	20.25
18.00	10.27	14.96	19.55
18.40	9.79	14.40	18.80
18.80	9.25	13.75	17.96
19.20	8.66	13.00	17.06
19.60	7.97	12.12	16.06
20.00	7.00	11.06	14.95

Effect of Coefficient of Friction on Blade Cutting Force (kN)

	Coefficient of friction			
Displacement (mm)	**0.05**	**0.1**	**0.2**	**0.3**
0.00	0.00	0.00	0.00	0.00
0.60	3.68	3.68	3.69	3.69
1.20	6.28	6.31	6.31	6.32
1.80	8.31	8.36	8.43	8.44
2.40	10.04	10.14	10.25	10.28
3.00	11.56	11.70	11.87	11.92
3.60	12.90	13.08	13.31	13.38
4.20	14.10	14.33	14.62	14.72
4.80	15.19	15.46	15.82	15.96
5.40	16.17	16.50	16.92	17.09
6.00	17.08	17.45	17.94	18.15
6.60	17.91	18.33	18.90	19.14
7.20	18.67	19.14	19.78	20.07
7.80	19.36	19.88	20.61	20.94
8.40	20.00	20.57	21.39	21.75
9.00	20.58	21.20	22.12	22.51
9.60	21.10	21.77	22.80	23.23
10.20	21.58	22.29	23.43	23.90
10.80	22.00	22.77	24.01	24.52
11.40	22.38	23.19	24.54	25.11
12.00	22.71	23.57	25.03	25.65
12.60	22.99	23.90	25.46	26.15
13.20	23.22	24.18	25.85	26.61
13.80	23.41	24.42	26.19	27.04
14.40	23.56	24.60	26.49	27.43
15.00	23.66	24.74	26.73	27.78

	Coefficient of friction			
Displacement (mm)	**0.05**	**0.1**	**0.2**	**0.3**
15.60	23.71	24.83	26.93	28.10
16.20	23.73	24.87	27.07	28.37
16.80	23.71	24.86	27.15	28.62
17.40	23.65	24.80	27.16	28.81
18.00	23.55	24.70	27.09	28.95
18.60	23.42	24.56	26.95	29.02
19.20	23.24	24.36	26.75	29.02
19.80	23.03	24.13	26.50	28.96
20.40	22.78	23.86	26.19	28.79
21.00	22.48	23.55	25.83	28.50
21.60	22.14	23.19	25.42	28.10
22.20	21.76	22.79	24.96	27.60
22.80	21.34	22.35	24.45	27.02
23.40	20.87	21.86	23.88	26.36
24.00	20.35	21.32	23.25	25.64
24.60	19.78	20.71	22.56	24.86
25.20	19.15	20.04	21.82	24.01
25.80	18.46	19.30	21.00	23.09
26.40	17.68	18.49	20.11	22.10
27.00	16.80	17.59	19.13	21.02
27.60	15.79	16.59	18.06	19.86
28.20	14.58	15.46	16.88	18.59
28.80	13.20	14.15	15.58	17.20
29.40	11.59	12.62	14.19	15.78
30.00	8.75	10.16	12.15	13.85

BIBLIOGRAPHY

ABAQUS Analysis User's Manual Ver. 6.10, Dassault Systems Inc., Providence, RI, USA 2010.

Abo-Elnor, M. E. (2002), Advanced Numerical Techniques to Simulate Soil-tool Interface Problems, PhD. Dissertation, University of Strathclyde, Egypt, 312 pp.

Abo-Elnor, M. E., El-Aziz, S. M. A. and Shokry, M. K. (1998), "Experimental Study of Blade-soil Interaction Forces," In Proceedings of the 8th International Applied Mechanics and Mechanical Engineering Conference, Cairo, Egypt.

Altair Hyperworks, HyperMesh User's Manual, Version 10.0, Altair Engineering, Troy, MI, USA, 2009.

Anim, K. (2010), Effect of Strain Rate on the Shear Strength of Questa Rock Pile Materials, MS Thesis, New Mexico Institute of Mining and Technology, Socorro, NM, USA, 99 pp.

Araya, K. and Gao, R. (1995), "A Non-Linear Three Dimensional Finite Element Analysis of Subsoiler Cutting with Pressurized Air Injection," *Journal of Agricultural Engineering Research, Vol. 61*, pp. 115-128.

Asaf, Z., Rubinstein, D. and Shmulevich, I. (2007), "Determination of Discrete Element Model Parameters required for Soil Tillage," *Soil and Tillage Research, Vol. 92(1-2),* pp. 227-242.

Atkinson, J. H. and Bransby, P. L. (1978), The Mechanics of Soils: An Introduction to Critical State Soil Mechanics, McGraw Hill, London.

Awuah-Offei, K. (2005), Dynamic Modeling of Cable Shovel-Formation Interactions for Efficient Oil Sands Excavation, PhD. Dissertation, Missouri University of Science and Technology, Rolla, MO, USA, 147 pp.

Bailey, A. C., Johnson, C. E. and Schafer. R. L. (1984), "Hydrostatic Compaction of Agricultural Soils," *Transaction of ASAE, Vol. 27(4),* pp. 952-955.

Bathe, K. J., Bolourchi, S., Ramaswamy, S. and Snyder, M. D. (1978), "Some Computational Capabilities for Nonlinear Finite Element Analysis," *Nuclear Engineering and Design, Vol. 46(2),* pp. 429-455.

Bathe, K. J. and Cimento, A. P. (1980), "Some Practical Procedures for the Solution of Nonlinear Finite Element Equations," *Computer Methods in Applied Mechanics and Engineering, Vol. 22(1),* North-Holland Publishing Company, pp. 59-85.

Bathe, K. J., Ramm, E. and Wilson, E. L. (1973), "Finite Element Formulations for Large Deformation Dynamic Analysis," *International Journal of Numerical Methods in Engineering, Vol. 9,* pp. 353-386.

Becker, A. A. (2004), An Introductory Guide to Finite Element Analysis, The American Society of Mechanical Engineers, New York, 167 pp.

Brinkgreve, R. B. J. (2005), "Selection of Soil Models and Parameters for Geotechnical Engineering Application," *In Geotechnical,* eds. Yamamuro, J. A. and Kaliakin, V. N.,. ACSE, No.128, pp. 69-98.

Callari, C., Auricchio, F. and Sacco, E. (1998), "A Finite-strain Cam-clay Model in the Framework of Multiplicative Elasto-plasticity," *International Journal of Plasticity, Vol. 14(12),* pp. 1155-1187.

Chi, L. and Kushwaha, R. L. (1989), "Finite Element Analysis of Forces on a Plane Soil Blade," *Canadian Agriculture Engineering, Vol. 31(2),* pp. 135-140.

Chi, L. and Kushwaha, R.L. (1990), "A Non-Linear 3-D Finite Element Analysis of Soil Failure with Tillage Tools," *Journal of Terramechanics, Vol. 27(4),* Elsevier Science Ltd., UK, pp. 343-366.

Chi, L. and Kushwaha, R. L. (1991), "Three-dimensional Finite Element Interaction between Soil and Simple Tillage Tool," *Transactions of the ASAE, Vol. 34(2),* pp. 361-366.

Chi, L., Kushwaha, R. L. and Shen, J. (1993), "An Elasto-plastic Constitutive Model for Agricultural Cohesive Soil," *Canadian Agriculture Engineering, Vol. 35(4),* pp. 245-251.

Coulomb, C. A. (1776), "Essai sur une application des regles des maximis et minimis a quelques problemes de statique relatives a l'architecture:, *Academic Royal des Sciences: Memoires de Mathematique et de Physique*, presents a l'Academie Royale des Sciences, par Divers Savants, et lus dans les Assemblees, Paris, Vol. 7, pp. 343-382.

Dafalias, Y. F. (1993). "Overview of constitutive models used in VELACS," *International Conference on Verification of Numerical Procedures for the analysis of soil liquefaction problems, Vol. 2,* Balkema, Rotterdam, pp. 1293-1304.

Davoudi, S., Alimardani, R., Keyhani, A. and Atarnejad, R. (2008), "A Two-dimensional Finite Element Analysis of a Plane Tillage Tool in Soil using a Non-linear Elasto-Plastic Model," *American-Eurasian Journal of Agricultural and Environmental Science, Vol. 3(3),* pp. 498-505.

Drucker, D. C. (1953), "Limit Analysis of Two and Three dimensional Soil Mechanics Problems," *Journal Mechanics and Physics of Solids, Vol. 1(4),* pp. 217-226.

Drucker, D. C., Gibson, R. E. and Henkel, D. J. (1957), "Soil Mechanics and Work Hardening Theories of Plasticity," *Transaction of ASCE, Vol. 122*, pp. 338-346.

Drucker, D. C. and Prager, W. (1952), "Soil Mechanics and Plastic Analysis for Limit Design," *Quarterly of Applied Mathematics, Vol. 10*, pp. 157-165.

Duncan, J. M. (1994), "The Role of Advanced Constitutive Relations in Practical Applications," *Proceeding of the 13th International Conference on Soil Mechanics and Foundation Engineering, Vol. 5*, New Delhi, India, pp. 31-48.

Duncan, J. M. and Chang, C. Y. (1970), "Nonlinear Analysis of Stress and Strain in Soil," *Journal of the Soil Mechanics and Foundations Division, ASCE, Vol. 96(SM5),* pp. 1629-1653.

Fielke, J.M. (1999), "Finite Element Modeling of the Interaction of the Cutting Edge of Tillage Implements with Soil," *Journal of Agricultural Engineering Research, Vol. 74*, pp. 91-101.

Frimpong, S. and Hu, Y. (2008), "Intelligent cable shovel excavation modeling and simulation," *Internal Journal of Geomechanics, Vol. 8(1)*, pp. 1-10.

Gens, A. and Potts, D. M. (1988), "Critical State Models in Computational Geomechanics," *Engineering Computations, Vol. 5(3),* pp. 178-197.

Helwany, S. (2007), Applied Soil Mechanics: With ABAQUS Applications, John Wiley and Sons, Inc., Hoboken, New Jersey.

Hemani, A., Goulet, S. and Aubertin, M. (1994), "Resistance of Particulate Media Excavation: Application to Bucket Loading," *International Journal of Surface Mining, Reclamation and Environment, Vol. 8(3),* A. A. Balkema, Rotherdam, Netherlands, pp. 125-129.

Hemami, A. and Hassani, F. (2007), "Simulation of the Resistance of Bulk Media to Bucket in a Loading Process," 24th International Symposium on Automation & Robotics in Construction, Construction Automation Group, I.I.T. Madra, India, pp. 163-168.

Karafiath, L.L., and Nowatzki, E.A. (1978), Soil Mechanics for Off-Road Vehicle Engineering, Trans Tech Publications, Clausthal, West Germany.

Karmakar, S., Sharma, J. and Kushwaha, R. L. (2004) "Critical State Elasto-plastic Constitutive Models for Soil Failure in Tillage – A Review," *Canadian Biosystems Engineering, Vol. 46,* pp. 2.19-2.23.

Kondner, R. L. and Zelasko, J. S. (1963), "A Hyperbolic Stress-strain Response: Cohesive Soil," *Journal of the Soil Mechanics and Foundations Division, ASCE, Vol. 89(SM1),* pp. 115-143.

Kumari, D. (2009), Effect of Moisture on Strength Characteristics of river sand, Bachelor's Thesis, Department of Civil Engineering, National Institute of Technology, Rourkela, India.

Kushwaha, R. L. and Shen, J. (1994), "The Application of Plasticity in Soil Constitutive Modeling," *ASAE Paper No. 941072,* St Joseph, MI,ASAE.

Kushwaha, R. L. and Shen, J. (1995a). "Numeric Simulation of Friction Phenomenon at Soil-Tool Interface," *Tribology Transactions, Vol. 38(2),* pp. 424-430.

Kushwaha, R. L. and Shen, J. (1995b). "Finite Element Analysis of the Dynamic Interaction between Soil and Tillage Tool," *Transactions of the ASAE, Vol. 38(5),* pp. 1315-1319.

Kushwaha, R.L. and Zhang, Z.X. (1998), "Evaluation of Factors and Current Approaches Related to Computerized Design of Tillage Tools: A Review," *Journal of Terramechanics, Vol. 35(2),* pp. 69 – 86.

Lade, P. V. and Nelson, R. B. (1984), "Incrementalization Procedure for Elasto-plastic Constitutive Model with Multiple, Intersecting Yield Surface," *International Journal for Numerical and Analytical Methods in Geomechanics, Vol. 8(4),* pp. 311-323.

Martin, C. L., Favier, D. and Suery, M. (1997), "Viscoplastic Behaviour of Porous Metallic Materials Saturated with Liquid Part I: Constitutive Equations," *International Journal of Plasticity, Vol. 13(3),* pp. 215-235.

McKyes, E. and Ali, O. S. (1977), "The Cutting of Soil by Narrow Blades," *Journal of Terramechanics, Vol. 14(2),* pp. 43 – 58.

Momozu, M., Oida, A., Yamazaki, M. and Koolen, A. J. (2003), "Simulation of a Soil Loosening Process by Means of the Modified Distinct Element Method," *Journal of Terramechanics, Vol. 39,* Elsevier Science Ltd., UK, pp. 207-220.

Mouazen, A. M. and Nemenyi, M. (1999), "Finite Element Analysis of Subsoiler Cutting in Non-homogeneous Sandy Loam Soil," *Soil and Tillage Research, Vol. 51(1-2),* pp. 1-15.

NMA (2004), "Facts of Coal and Minerals," © NMA, Constitution Ave. NW, Washington D.C. 20001. http://www.nma.org/publications/facts_about.asp.

Osman, M. S. (1964), "The Mechanics of Soil Cutting Blades," *Journal of Agricultural Engineering Research, Vol. 9(4),* Elsevier Science Ltd., New York, USA pp. 313-328.

Payne, P. C. J. (1956), "The Relationship between the Mechanical Properties of Soil and the Performance of Simple Cultivation Implements," *Journal of Agricultural Engineering Research, Vol. 1 (1),* Elsevier Science Ltd., New York, NY, USA, pp. 23-50.

Payne, P. C. J. and Tanner, D. W. (1959), "The Relationship between Rake Angle and the Performance of Simple Cultivation Implements," *Journal of Agricultural Engineering Research, Vol. 4(4),* Elsevier Science Ltd., New York, NY, USA, pp. 312-325.

Perumphral, J. V., Grisso, R. D. and Desai, C. S. (1983), "A Soil-Tool Model Based on Limit Equilibrium Analysis," *Transactions of the ASAE, Vol. 26(4),* American Society of Agricultural Engineers, St. Joseph, MI, USA, pp. 991-995.

Plouffe, C., Laguë, C., Tessier, S., Richard, M. J. and McLaughlin, N. B. (1999), "Mouldboard Plow Performance in a Clay Soil: Simulations and Experiment," *Transactions of ASAE, Vol. 42(6),* pp. 1531-1539.

Pollock, D. Jr., Perumpral, J. V. and Kuppusamy, T. (1986), "Finite Element Analysis of Multipass Effects of Vehicles on Soil Compaction," *Transactions of ASAE, Vol. 29(1),* pp. 45-50.

Potts, D. M. and Zdravkovic, L. (1999), Finite Element Analysis in Geotechnical Engineering, ThomasTelford Publishing, London.

Rankine, W. (1857), "On the Stability of Loose Earth," *Philosophical Transactions of the Royal Society of London, Vol. 147,* pp. 9-27.

Reece, A. R. (1965), "The Fundamental Equation of Earthmoving Mechanics," *Symposium on Earthmoving Machinery*, Institute of Mechanical Engineers, 179, Part 3 F, London, UK.

Rosa, U. A. and Wulfsohn, D. (1999), "Constitutive Model for High Speed Tillage using Narrow Tools," *Journal of Terramechanics, Vol. 36(4)*, pp. 221-234.

Roscoe, K. H. and Burland, J. B. (1968), "On the Generalized Stress-strain Behavior of Wet Clay," *In Engineering Plasticity*, eds. Heyman, J. and Leckie, F. A, Cambridge, England, Cambridge University Press, pp. 535-609.

Roscoe, K. H. and Schofield, A. N. (1963), "Mechanical Behavior of an Idealized Wet Clay," Proceedings European Conference on Soil Mechanics and Foundation Engineering, Wiesbaden (Essen: Deutsche Gesellschaft fur Erd-und Grundbau e.V.), Vol. 1, pp. 47-54.

Roscoe, K. H., Schofield, A. N. and Wroth, C. P. (1958), "On the Yielding of Soils," *Géotechnique, Vol. 8(1)*, pp. 22-53.

Saada, R. A., Bonnet, G. and Bouvard, D. (1996), "Thermomechanical Behavior of Casting Sands: Experiments and Elasto-plastic Modeling," *International Journal of Plasticity, Vol. 12(3)*, pp. 273-294.

Schanz, P. Vermeer, A. and Bonnier, P. G., (1999) "The Hardening Soil Model: Formulation and Verification," *in Proceedings of the International Symposium Beyond 2000 in Computational Geotechnics*, Balkema, Rotterdam, pp. 281–296.

Schofield, A. N. and Wroth, C. P. (1968), Critical State Soil Mechanics, London, McGraw-Hill.

Shen, J. and Kushwaha, R. L. (1998), Soil-Machine Interactions: A Finite Element Perspective, Marcel Decker, Inc, New York, NY.

Shen, J. and Kushwaha, R. L. (1995), "Investigation of an Algorithm for Nonlinear and Dynamic Problems in Soil-machine Systems," *Computers and Electronics in Agriculture, Vol. 13*, pp. 51-66.

Shield, R. T. (1955), "On Coulomb's Law of Failure in Soils," *Journal of Mechanics and Physics of Solids, Vol. 4(1)*, pp. 10-16.

Soehne, W. (1956), "Some Principle of Soil Mechanics as applied to Agricultural Engineering," *Grundlagen der landtechnik, Vol. 7*, National Inst. Agric. Eng. Translation 53, pp. 11-27.

Swick, W. C. and Perumpral, J. V. (1988), "A Model for Predicting Soil-Tool Interaction," *Journal of Terramechanics, Vol. 25*, Elsevier Science Ltd., UK, pp. 43-56.

Tanaka, H., Momozu, M., Oida, A. and Yamazaki, M. (2000), "Simulation of Soil Deformation and Resistance at Bar Penetration by the Distinct Element Method," *Journal of Terramechanics, Vol. 37*, Elsevier Science Ltd., UK, pp. 47-56

Terzaghi, K., Peck, B. R., and Mesri, G. (1996), "Soil Mechanics in Engineering Practice," 3rd ed., Wiley, New York, pp 71-213.

Tons, M., Doerfler, M., Meinecke, M. and Obojski, M. A. (2004), "Radar Sensors and Sensor Platform used for Pedestrian Protection in the EC-funded Project SAVE-U," IEEE Intelligent Vehicle Symposium, Parma, Italy, June, 14-27, pp. 813-818.

Ura, T. and Yamamoto, Y. (1978), "Stability of Dragged Anchors," *Institute of Industrial Science: The University of Tokyo, Vol. 24(4),* Published Minato-Ku, Tokyo, Japan, pp. 1-19.

Wilkinson, A. and DeGennaro, A. (2007), "Digging and Pushing Lunar Regolith: Classical Soil Mechanics and the Forces needed for Excavation and Traction," *Journal of Terramechanics, Vol. 44*, Elsevier Science Ltd., UK, pp. 133-152.

Wood, D. M. (1990), Soil Behavior and Critical State Soil Mechanics, Cambridge University Press, Cambridge, England.

Wroth, C. P. (1975), The Predicted Performance of Soft Clay under a Trial Embankment Loading based on the Cam-clay Model, In Finite Elements in Geomechanics, John Wiley and Sons, London, pp. 191-208.

Wroth, C. P. and Houlsby, G. T. (1985), "Soil Mechanics-property Characterization and Analyzes Procedures," *In Proceedings of the 11th International Conference SMFE, Vol. 1*, San Francisco, pp. 1-55.

Yong, R. N. and Hanna, A.W. (1977), "Finite Element Analysis of Plane Soil Cutting," *Journal of Terramechanics, Vol. 14(3),* Elsevier Science Ltd., UK, pp. 103-125.

Zelenin, A. N., Balovnev, V. I., and Kerov, I. P. (1985), Machines for Moving the Earth: Fundamentals of the Theory of Soil Loosening, Modeling of Working Processes and Forecasting Machine Parameters, A. A. Balkema, Rotherdam, Netherlands, 555 pp.

Zeng, D. and Yao, Y. (1992), "A Dynamic Model for Soil Cutting by Blade and Tine," *Journal of Terramechanics, Vol. 29(3),* Elsevier Science Ltd., UK, pp. 317-327.

VITA

Osei Frempong Brown was born on August 2, 1982 in Ghana, West Africa. He received his BS in Mining Engineering (first class honors) in May 2006, from Kwame Nkrumah University of Science and Technology's School of Mines (since renamed the University of Mines and Technology), Ghana. He worked as a summer intern in 2005 with AngloGold Ashanti Obuasi Mine, Ghana. In 2006, he joined AngloGold Ashanti Iduapriem Mine, Ghana as a Mining Engineer. He has studied under the guidance of Dr. Samuel Frimpong since 2008 at Missouri University of Science and Technology. During the summer of 2011, he worked with Peabody Energy's North Antelope Rochelle Mine, WY as a Mining Engineer.

Osei Frempong Brown is a member of the Society for Mining, Metallurgy and Exploration (SME) and the Canadian Institute of Mining, Metallurgy and Petroleum (CIM).